IMPI's 49TH ANNUAL MICROWAVE POWER SYMPOSIUM (IMPI 49)

2015 PROCEEDINGS

June 16-18, 2015

Kona Kai Resort
San Diego, California, USA
www.IMPI.org

ISSN: 1070-0129

Presented by the
INTERNATIONAL MICROWAVE POWER INSTITUTE
PO Box 1140, Mechanicsville, VA 23111
Phone: +1 (804) 559 6667 • Email: info@impi.org
WWW.IMPI.ORG

Welcome to San Diego for the 49th IMPI Symposium

Each year, IMPI brings together researchers from across the globe to share the latest findings in microwave and RF heating theories and applications, and this year we have an outstanding array of researchers in attendance. If you are not yet a member of IMPI, we strongly encourage you to consider joining onsite. IMPI membership connects you to microwave and RF academia, researchers, developers and practitioners across the globe. Talk to an IMPI member today to learn more about the value of joining our outstanding organization!

Thank you for joining us. We hope you learn from the technical presentations, interact with your colleagues, and enjoy the atmosphere of the Symposium. And do take the opportunity to visit the many interesting sites in and around San Diego.

Special thanks to the following partners for printing these Proceedings:

LIVERPOOL JOHN MOORES UNIVERSITY

Built Environment & Sustainable Technologies BEST Research Institute

IMPI wishes to express its gratitude to the following individuals:

TECHNICAL PROGRAM COMMITTEE

Chair Raymond Boxman, Tel Aviv University, Israel
Co-chair Ulrich Erle, Nestle R & D, USA

Members
Kadir Aslan, Morgan State University, USA
Vladimir Bilik, S-TEAM Lab, Slovakia
Georgios Dimitrakis, University of Nottingham, UK
John F. Gerling, GAE, Inc., USA
Marilena Radoiu, SAIREM, France
Bob Schiffmann, R.F. Schiffmann Associates, Inc., USA
Yasunori Tanaka, Kanazawa University, Japan
Vadim V. Yakovlev, Worcester Polytechnic Institute, USA

FOOD SCIENCE AND TECHNOLOGY COMMITTEE

Chair Jeyamkondan Subbiah, University of Nebraska-Lincoln, USA

Members
Justin Balousek, Heinz, USA
Corey Crooks, Graphic Packaging International, USA
Sumeet Dhawan, Nestle R & D, USA
Marie Jirsa, Tyson Foods, USA
Ric Gonzalez, ConAgra Foods, USA
Shyam Sablani, Washington State University, USA
K.P. Sandeep, N.C. State University, USA
Juming Tang, Washington State University, USA
Mark Watts, Campbell Soup Company, USA

Purchasing Information: Copies of the Proceedings of the 49th Annual Microwave Power Symposium, as well as back issues from prior years, are available for purchase. Contact Molly Poisant, Executive Director of IMPI, at +1 804 559 6667 or molly.poisant@impi.org for details.

Table of Contents

Food & Agriculture

Table of Contents

Materials, Chemicals, Plasma & Properties

Table of Contents

Components & Systems

Microwave Induced Plasmas and Their Applications in the Food Industry

K.-D. Weltmann, M. Andrasch, M. Baeva, A. Boesel, U. Schnabel and J. Ehlbeck

Leibniz-Institut for Plasma Science and Technology e. V., Greifswald, Germany

Keywords: microwave plasma, sanitation, decontamination, food preservation

INTRODUCTION

Gentle sanitation of fresh fruits and vegetables is highly demanded since consumption of raw food products entails risk of food-borne illnesses. Recent outbreaks in Western Europe involved EHEC (enterohemorrhagic *Escherichia coli*) on sprouts, *Listeria monocytogenes* on meat and norovirus in frozen strawberries. Currently used disinfection or sanitation methods for fresh fruits and vegetables lack antimicrobial effectiveness, are costly and consume water or chemicals. Non-thermal atmospheric pressure microwave plasma offers a promising opportunity for fresh food preservation. Accordingly over the last decade, different microwave plasma sources were developed and optimized to meet health requirements without decreasing product quality. In addition, methods for the decontamination of packaging materials were established and a system for detecting traces of mercury was developed. This contribution overviews food and packaging decontamination by microwave plasmas.

METHODOLOY

The antimicrobial effects of plasma are well known and investigated for different types of plasma sources, which can be driven for instance by microwaves at 2.45 GHz. An adjustment-free ignition structure was developed to ignite at atmospheric pressure a volume plasma with less than 2 kW power. The induced plasma could be applied by different methods for sanitation. Thermolabile (e.g. hollow) packaging materials, PET bottles, were directly treated by placing them inside a microwave chamber in which plasma was ignited. Barrier-free access for these PET-bottles was provided by special microwave tunnels (figure 1b).

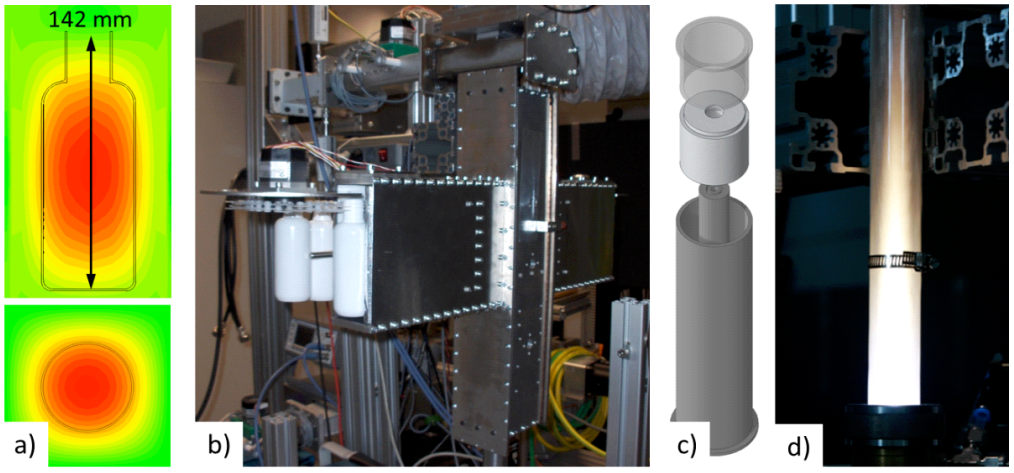

Figure 1. Distribution of the electric field strength (a) inside the reactor (b) for decontamination of PET-bottles. Sketch of the PLexc® plasma torch (c) and a photograph of the ignited plasma (d).

Plasma and its reactive species was also applied indirectly with a PLexc® plasma torch (figure 1c) attached to a reaction chamber. After igniting the plasma (figure 1d), the long-lifetime reaction products were used for different sanitation applications. This approach minimizes heating of the treated products.

RESULTS

Decontamination of the PET-bottles with the direct microwave plasma treatment reduced *Bacillus atropheus* by about 6 orders of magnitude (figure 2a). This inactivation was achieved without exceeding the maximum temperature of PET-bottles of about 60 °C [1-2]. The inactivation of different microorganisms on apples with the indirect treatment also reached 6 orders of magnitude for a variety of different microorganisms. A preliminary sensory study showed no direct correlation between plasma treatment and examined product properties [3].

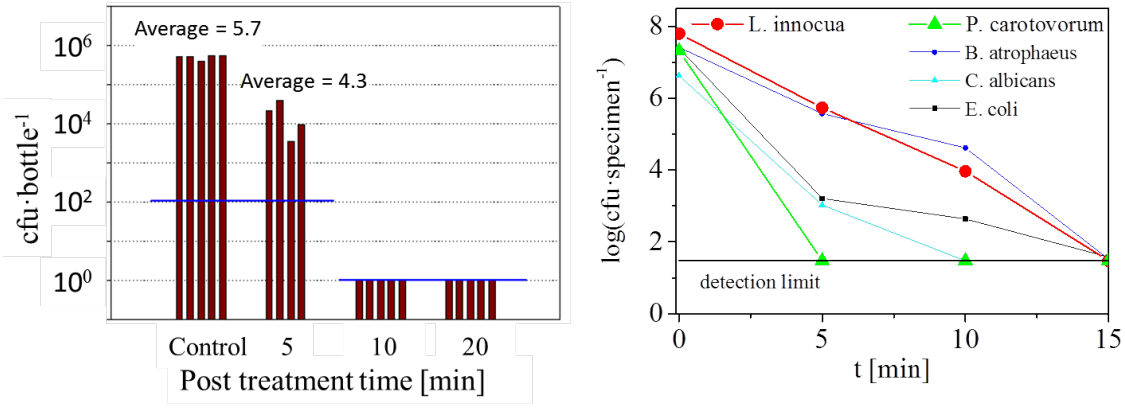

Figure 2. (a) Direct plasma inactivation in PET-bottles. (b) Inactivation kinetics of different microorganisms with indirect treatment of apples.

CONCLUSION

Depending on the product, atmospheric pressure microwave plasma can be applied directly or indirectly. Both methods effectively and economically decontaminate packaging materials and sanitize food.

REFERENCES

[1] Ehlbeck J, Brandenburg R, von Woedtke T, Krohmann U, Stieber M and Weltmann K-D "Plasmose - antimicrobial effects of modular atmospheric plasma sources" *GMS Krankenhaushygiene Interdisziplinär* 2008 **3** 12pp

[2] Ehlbeck J, Schnabel U, Polak M, Winter J, Woedtke T v, Brandenburg R, et al. "Low temperature atmospheric pressure plasma sources for microbial decontamination" *Journal of Physics D: Applied Physics* 2011 **44** 33pp

[3] Schnabel U, Niquet, R., Schlüter, O., Gniffke, H., Ehlbeck, E. "Decontamination and sensory properties of microbiologically contaminated fresh fruits and vegetables by microwave plasma processed air (PPA)" *Journal of Food Processing and Preservation* 2014 10pp

Development of Microwave Pasteurization Processes for Packaged Foods

Frank Liu[1], Tom Yang[2], Juming Tang[1], Donglei Luan[1], Feng Li[1], Zhongwei Tang[1], Huiming Lin[1] and Stewart Bohnet[1]

[1] Department of Biological Systems Engineering, Washington State University, Pullman, WA 99164-6120, USA
[2] US Army Natick Soldier Systems Center, 14th Avenue, Natick, MA 01760, USA

Keywords: Microwave heating, pasteurization, processing schedule, sensory tests, heating pattern, model food.

INTRODUCTION

A 915 MHz single mode microwave assisted pasteurization system (MAPS™) was developed to produce refrigerated food products with better quality and nutrition attributes compared with the traditionally thermal processed foods [1]. The main challenge is to develop a process in which the cold spots should be heated to reach the desired temperature for inactiviction of target pagethens. The objectives of this study were to develop microwave (MW) pasteurization processes for heterogeneous foods, such as buffalo chicken salad, deviled egg potato salad and macaroni and cheese packaged in 10.5-oz trays. The sensory tests and microbial challenge studies or the MW processed food products using MAPS were also conducted to evaluate the influence of the process and storage conditions on product sensory attributes.

METHODOLOY

A 15-kW, 915-MHz, single-mode, semi-continuous MW assisted pasteurization system was used for this study (Fig. 1 (a)). Gellan gel with appropriate composition was used as the model food to emulate the real food for heating pattern and cold spot detection. The heating pattern and cold spot were determined by a chemical-marker assisted computer-vision method. The identified cold spot was confirmed as the actual cold spot in the food trays by directly measuring temperatures at cold regions using mobile temperature sensors inside real food trays during processing. Heat penetration tests were then conducted in which temperature at the cold spot inside the food trays was measured by temerpature sensor. MW processing schedules for pasteurization of three food products were developed based on the heat penetration tests.

RESULTS

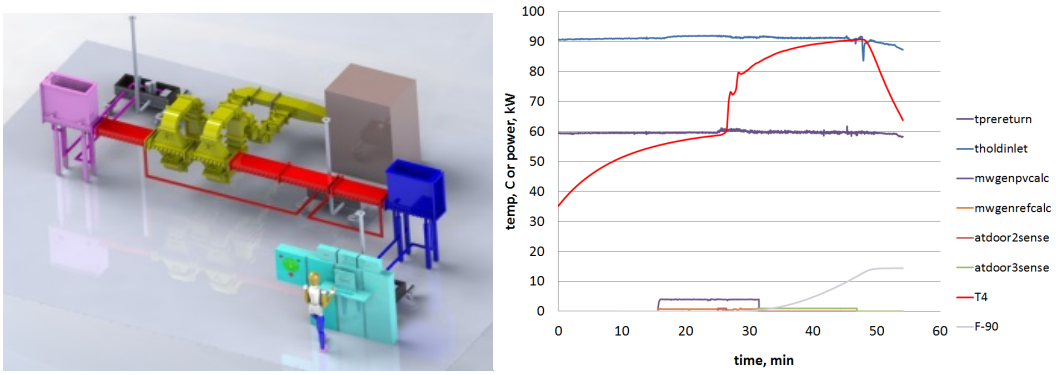

(a) (b)

Figure 1. (a) 20-kW, 915-MHz, single-mode, semi-continuous MW assisted pasteurization system (b) Temperature profile measured at the location of cold spot in 10.5 oz. macaroni and cheese tray.

Figure 1 (b) shows the temerpature history at the cold spot in food trays during microwave pasteurization of pre-packaged macaroni and cheese in MAPS. The developed processing schedules are effective for the MW pasteurization of prepackaged foods. This was confirmed by preliminary processing tests on macaroni and cheese, buffalo chicken salad and deviled egg potato salad with F_{90} = 10 min schedule. The processed samples were produced for the sensory tests.

DISCUSSION

Temperature history at the cold spot in food trays indicated that the 915-MHz single-mode semi-continuous MW- pasteurization technology is effective for processing of heterogeneous foods packaged in trays. The MW pasteurization method is technically feasible for production of other refrigerated packaged heterogeneous foods. Samples were sent for microbial enumeration The results show no positive detection of food pathogens in the processed foods.

CONCLUSION

Uniform microwave heating of pre-packaged heterogeneous foods can be achieved by proper selection of microwave power and heating time with MAPS. Mirowave pasturized food products are safe and have a good quanlity.

REFERENCES

[1] W. Zhang, F. Liu, C. Nindo, J. Tang, Physical properties of egg whites and whole eggs relevant to microwave pasteurization, J. Food Eng., 118 (2013), pp. 62–69.

Radio Frequency Treatment for Improved Stability of Rice Bran

Bo-Han Chen, Jian-De Lin, Yu-Fen Yen, Su-Der Chen*

National Ilan University, I-Lan City, Taiwan

Keywords: radio frequency, rice bran, lipase

INTRODUCTION

Rice bran is a by-product of rice milling, representing about 10% of a whole rice grain. However the activity of lipase in rice bran is very high, accelerating lipid oxidation and quality deterioration. Microwave heating inactivates lipase and can, together with vacuum packaging and low temperature storage, stabilize rice bran and extend the storage time [1-2]. The advantages of radio-frequency (RF) are longer wavelength and deeper penetration than microwaves; therefore it shows rapid and uniform heating. [3] The objective of this study was to establish radio frequency heating conditions for lipase inactivation in rice bran and to achieve quality stability of rice bran during room temperature storage.

METHODOLOY

Rice bran

Rice bran was purchased from Dongshan Township Farmers' Association. (Ilan, Taiwan)

RF system

A 5 kW, 40.68 MHz pilot-scale RF system (Model RB105, Dr-agriculture Inc., Taipei, Taiwan) was used in this study. The size of the parallel electrode plates was 35 cm x 35 cm. Different heating rates were obtained by adjusting the gap between the electrodes from 5 to 15 cm. The temperature profiles of packaged 1kg rice bran after RF treatments were measured by IR sensor at three different locations and the surface temperature distributions by thermal imager.

Quality analysis of RF treated rice bran during 25^{o}C storage

The rice bran was heated by RF for 2 min with 6 cm electrode gap and then immediately stored at room temperature (25^{o}C) for 4 weeks. The rice bran was analyzed lipase activity, acid value (CNS 3647 N6082), free fatty acid, peroxide value (CNS 3650-N6085), color (Hunter L.A.B Color Flex) and scavenging 1,1-diphenyl-2-picrylhydrazyl (DPPH) radicals ability.

RESULTS AND DISCUSSIONS

The results show that decreasing RF electrode gap distance obtained high RF power. When the RF electrode plate gap was controlled at 6 cm, 1 kg rice bran required only 2 min to reach about 100°C and temperature distribution was uniform (Fig. 1). The retention of lipase activities was significantly reduced after RF treatment (Fig. 2). The RF treated rice bran had significantly lower acid value, free fatty acid content and peroxide value than un-RF treated rice bran at room temperature one to four weeks storage (Table 1). RF heated rice bran had less brightness and slight higher yellowness. However four weeks storage time didn't significantly change color and scavenging DPPH radical ability of rice bran.

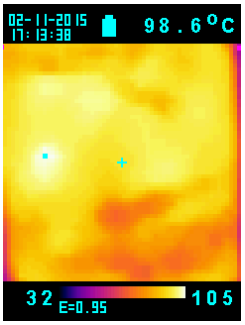

Fig. 1. Surface temperature distributions of 1kg rice bran after 2 min RF treatment.

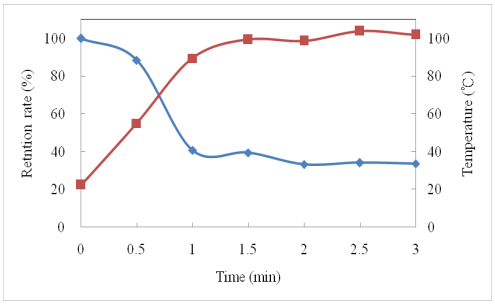

Fig. 2. Temperature profiles and change of lipase retention rates of rice bran during RF.

Table 1. Quality changes of the fresh and RF 2 min treated rice bran during 25°C storage.

Quality	weeks	0	1	2	3	4
Acid value	Fresh	6.35±0.05	17.28±0.16	21.62±0.15	20.62±0.11	20.87±0.08
	RF	5.74±0.02	7.25±0.06	7.59±0.04	7.62±0.02	7.93±0.07
Free fatty acid	Fresh	16.31±0.14	44.41±0.40	55.57±0.04	53.02±0.28	53.63±0.20
	RF	13.46±0.19	18.64±0.15	19.50±0.11	19.58±0.06	20.38±0.17
Peroxide value	Fresh	1.91	4.74±0.93	2.31±0.30	2.34±0.04	2.88±0.08
	RF	1.74	2.64±3.65	2.10±0.25	1.86±0.08	2.46±0.08
Scavenging DPPH (%)	Fresh	88.12±0.93	87.20±0.04	86.69±0.55	86.97±0.04	86.53±0.04
	RF	88.86±0.00	86.52±0.07	86.22±0.58	86.24±0.09	85.93±0.05

CONCLUSIONS

A 2-min RF treatment of 1 kg rice bran led to effective lipase inactivation; therefore it had significantly lower acid values, free fatty acids and peroxide values than untreated rice bran after several weeks of storage.

REFERENCES

[1] F.M. Ramezanzadeh, R.M. Rao, W. Prinyawiwatkul, W.E. Marshall and M. Windhauser, Effect of microwave heat, packaging and storage temperature on fatty acid and proximate compositions in rice bran, *J. Agric. Food Chem.*, vol. 48, pp. 464-467, 2000.

[2] J. Tao, R. Rao and J. Liuzzo, Microwave heating for rice bran tabilization. *J. Microw. Power Electromagn. Energy.*, vol. 28, no3, pp. 156-164, 1993.

[3] V. Orsat and G.S.V. Raghavan, Radio frequency processing. Emerging Technologies for Food Processing, San Diego: Academic Press, Inc. 446-468, 2005.

Microwave Dehydration of Vegetables

Xu Huibing[1] and Sirichai Songsermpong[2]

[1]School of Food Science and Technology, Jiangnan University, Wuxi, China
[2]Department of Food Science and Technology, Kasetsart University, Bangkok, Thailand

Keywords: Microwave, Vegetables, Dehydration, Moisture diffusivity, Quick rehydration

INTRODUCTION

Microwave dehydration has newly become an efficient dehydration method; it offers opportunities to shorten the drying time and improves the quick rehydration quality of dried products [1]. Microwave dehydration has high thermal efficiency and is easy to control. Therefore, it can reduce the operating cost for the food industry. Moreover, it is environmental friendly which is a strong point for doing business nowadays. The objective of this research was to understand the effect of microwave on drying of three vegetables, determine the moisture diffusivity and rehydration time and compare with traditional hot air drying.

METHODOLOGY

Carrots were peeled and cut into cubes of length 0.5 cm and cabbage leaves and snake beans were cut with a surface area of 1 cm^2 and 0.5 cm^2. Blanching time was determined by a peroxidase test. The vegetables were blached in boiling water with one percent salt and cooled immediately. The vegetables were dried in a continuous microwave oven with two magnetrons (2000 W) with different rounds of heating until the moisture content was less than 8% wb, the exposure time of one round was 30.7 s. The vegetables were also dried in a hot air drier at 60^oC and air velocity was 1 m/s for 150 min. The drying curves were plotted and the effective moisture diffusivities were determined using Fick's second law of diffusion for an infinite slab object [2]. The rehydration time was set to be 3 min in hot water 90^oC, the rehydrated product should absorb water and become fresh-like.

RESULTS

Suitable blanching times for carrot pieces, cabbage, and snake beans were 30 s, 2 min and 3 min, respectively. The effective moisture diffusivities of carrot were 5.5×10^{-7} m^2/s for microwave drying and 1.1×10^{-7} m^2/s for hot air drying. The effective moisture diffusivities of snake bean were 7.4×10^{-7} m^2/s for microwave drying and 1.3×10^{-7} m^2/s for hot air drying. The effective moisture diffusivities for cabbage were 4.1×10^{-8} m^2/s for microwave drying and 1.1×10^{-8} m^2/s for hot air drying. It took 120 min to dry carrots by hot air drying while it took only 21.3 min by microwave drying.

DISCUSSION

Microwave drying is 4-6 times faster than traditional hot air drying due to the volumetric heating while the hot air drying uses convection and conduction heat transfer which is slow.

CONCLUSION

The drying time was reduced by microwave drying by 76-82%. The rehydration time was also rapid in hot water for 3 min with good quality.

REFERENCES

[1] M. Zhang, J. Tang, A.S. Mujumdar and S. Wang, Trends in microwave-related drying of fruits and vegetables, Trends Food Sci. Tech., vol 17, no 10, pp. 524-534, 2006.
[2] J. Crank.1975. Mathematics of diffusion. 2nd ed. Clarendon Press. Oxford, UK. 414 pp.

Microwave Vacuum Extraction of Krill Oil

Hao-Chang Chang, Su-Der Chen*

National Ilan University, I-Lan City, Taiwan 26047

Keywords: microwave, extraction, krill, oil

INTRODUCTION

Krill oil contains large amounts of long-chain polyunsaturated fatty acids (LC-PUFAs, such as: DHA, EPA) that bound with phospholipids. LC-PUFAs is easily degraded by high temperature and oxidation during solvent extraction resulting in low oil extraction yield. Microwave heating can rapidly increase temperature and pressure in the cells rupture krill cells and the oil can be dissolved in ethanol to increase oil extraction yield and decrease extraction time. Microwave vacuum extraction can use a lower solvent temperature and avoid the oxidation of oxygen-sensitive components (OSC) such as: astaxanthin, DHA, EPA etc. [1-4].

METHODOLOY

Antarctic krill

Krill was mixed with 95% ethanol, and then homogenized (12000 rpm) for 1 min.

Microwave vacuum extraction

A 1.6 kW, 2450 MHz microwave vacuum extraction system with adjustable power, pump and cooling water condenser was used in this study (Fig. 1). The oil was extracted from the homogenized krill using 95% ethanol by microwave extraction and the DHA in the krill oil extract was analyzed. The effects of solid-solvent ratio (1:4, 1:6, 1:8, 1:10, and 1:12), pressure (76(no vacuum), 46, 36 and 26 (cm Hg)) on DHA content in krill after microwave extraction were investigated.

RESULTS AND DISCUSSIONS

Temperature decreased with lower pressure and less than 60 s was required to reach equilibrium during 300 W microwave vacuum extraction of krill (Fig. 2). Although the higher solid-liquid ratio produced a higher DHA yield, 1:8 was suitable for 300 W microwave extraction of krill (Fig. 3). The vacuum system had higher DHA yield than atomspheric condition during 300 W microwave extraction of krill (Fig. 4); therefore, lower temperature and oxygen concentration could avoid oil oxidation.

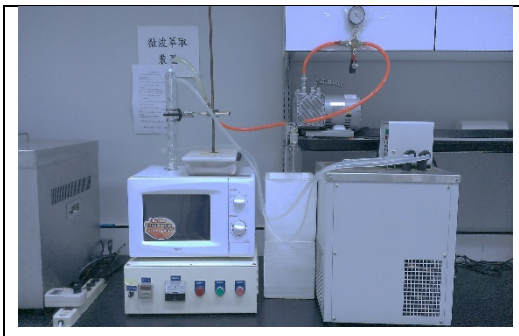

Fig. 1. Photograph of the microwave extraction system.

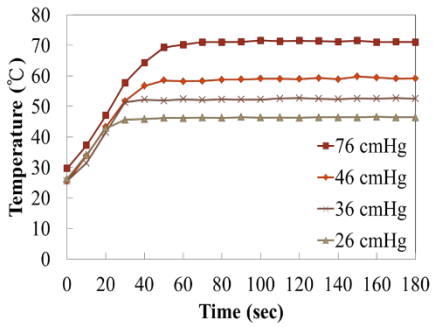

Fig. 2. Temperature-time history of krill duirng 200 W microwave-vacuum treatment at different pressures.

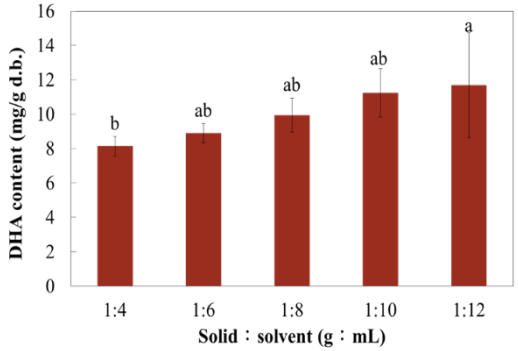

Fig. 3. Effect of solid-solvent ratio on DHA in krill by 300 W microwave extraction at 1 atm.

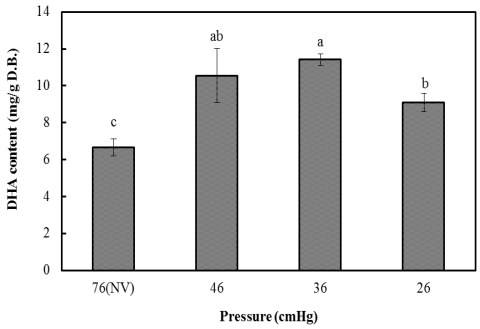

Fig. 4. Effect of pressure on DHA content krill after 300 W microwave vacuum extraction.

CONCLUSIONS

DHA extraction yield in krill increased with increasing solid-liquid ratio using 95% ethanol as solvent by 300 W microwave extraction. Microwave vacuum extraction can protect DHA against the damage of high temperature and oxidation during the process and enhance its extraction efficiency.

REFERENCES

[1] Zhao, L., Zhao, G. G., Chen, F., Wang, Z. F., Wu, J. H. & Hu, X. S. **(2006).** Different effects of microwave and ultrasound on the stability of (all-E)-astaxanthin. *J Agric Food Chem*, 54, 8346-8351.

[2] Wang, J. X. *et al.* (2008). Study of vacuum microwave-assisted extraction of polyphenolic compounds and pigment from Chinese herbs. *J Chromatogr A, 1198-1199*, 45-53.

[3] Xiao, X. *et al.* (2012). Microwave-assisted extraction performed in low temperature and in vacuo for the extraction of labile compounds in food samples. *Anal Chim Acta, 712*, 85-93.

[4] Xiao, X. H. *et al.* (2009). Evaluation of vacuum microwave-assisted extraction technique for the extraction of antioxidants from plant samples. *J Chromatogr A, 1216*(51), 8867-8873.

Heat and Mass Transport During Microwave Heating of Mashed Potato in Domestic Ovens – Model Development, Validation, and Sensitivity Analysis

J. Chen, K. Pitchai, S. Birla, M. Negahban, D. Jones, and J. Subbiah

University of Nebraska-Lincoln, Lincoln, USA

Keywords: microwave heating, heat and mass transfer, finite element method, modeling, sensitivity analysis.

INTRODUCTION

Computer simulation of the microwave heating process is becoming a powerful tool to help food scientists in developing food products, packages and cooking instructions that provide better cooking performance in domestic microwave ovens in terms of heating uniformity. Many models only simulated a short microwave heating time, such as 30 s, where the moisture movement and evaporation were not significant. For longer microwave heating duration, water evaporation is significant not only on the food surface but also inside the food product due to volumetric heating. A 3-D multiphase porous media microwave heating model using domestic microwave ovens has not been reported. Multiphase porous media models describing complex physical process, such as microwave heating in this study, require many input parameters. The objective of this work was to develop and validate a microwave heat-mass transfer model, and evaluate the effect of selected parameters on the predicted temperature profiles and total moisture loss.

METHODOLOY

A three-dimensional finite element model coupling electromagnetics and heat and mass transfer was developed to understand the interactions between the microwaves and fresh mashed potato in a 500 mL tray. The model was validated by heating mashed potato from 25 °C on a rotating turntable in a microwave oven, rated at 1200 W, for 3 minutes.

Several input parameters, such as the evaporation rate constant, the intrinsic permeability of water and gas, and the diffusion coefficient of water and gas, are not readily available for mashed potato, and they cannot be easily measured experimentally.

Reported values for raw potato were used as baseline values. A sensitivity analysis of these input parameters on the temperature profiles and the total moisture loss was evaluated by changing the baseline values to 10% and 1000% of the baseline values.

RESULTS AND DISCUSSION

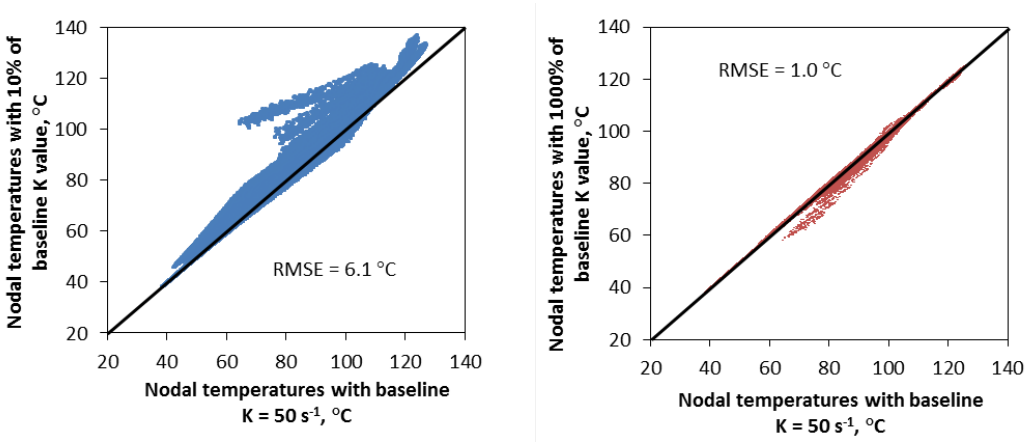

(a) 10% of baseline K value (b) 1000% of baseline K value

Figure 1. Sensitivity analysis of evaporation rate constant (k) on final nodal temperatures in the entire food domain.

The correlation of nodal temperatures between baseline model and those using different values of evaporation rate constant (k) is shown in a scatter plot (Figure 1). The nodal temperatures for k= 5 s^{-1} and k = 500 s^{-1} showed slight divergence from those for the baseline value of k at 50 s^{-1}. The Root-mean-square deviations were 6.1 and 1.0 °C, respectively, for k = 5 s^{-1} and k = 500 s^{-1}. Points along the diagonal line indicate that this parameter was not sensitive and vice versa. Also, most of the points falling in the upper triangle would indicate that the newer K value over-predicted the temperature, when compared to the baseline value, and vice versa. In general, the higher the value of K, the higher will be the rate of evaporation and therefore should result in lower overall nodal temperatures. The lower K value of 5 s^{-1} results in lower evaporation and higher overall temperatures by about 6.1 °C (most of data points fall in the upper triangle). Similarly, a higher K of 500 s^{-1} results in higher evaporation and lower overall temperatures by about 1.0 °C (most of the data points fall in the lower triangle).

CONCLUSION

The simulated spatial temperature profiles on the top and bottom layer of the mashed potato showed similar hot and cold spots when compared to the thermal images acquired by an infrared camera. Transient temperature profiles at six locations collected by fiber-optic sensors showed good agreement with predicted results, with the root-mean-square-error ranging from 1.6 to 11.7 °C. The predicted total moisture loss matched well with the observed result. The sensitivity analysis showed that, the gas diffusion coefficient, intrinsic water permeability, and the evaporation rate constant greatly influenced the predicted temperature and total moisture loss, while the intrinsic gas permeability and the water diffusion coefficient had little influence.

Development of Microwave Heating Instructions for Mashed Potato

Carol Valenzuela-Martinez, Mauricio Redondo-Solano, Jeyamkondan Subbiah and Harshavardhan Thippareddi

University of Nebraska, Lincoln, NE, USA

Keywords: microwave heating, mashed potato, *Salmonella* spp., validation

INTRODUCTION

Salmonella spp. is estimated to cause one million illnesses, 19,587 hospitalizations and 378 deaths in the United States annually [1]. The consumption of not ready-to-eat (NRTE) products prepared using microwaves ovens has been associated with salmonellosis infections. Non-uniform temperature distribution is a major issue with microwave heating of foods, causing *Salmonella* spp. survival. The objective of this study was to develop and validate microwave heating instructions for the destruction of *Salmonella* spp. in mashed potato using microwave ovens.

METHODOLOY

Two household microwave ovens (2.45 GHz frequency) were used: (1) 700 W (R-9470, SHARP Electronics, Mahwah, NJ) and (2) 1 350 W (JE51451DN1BB, General Electric Co., Louisville, KY).

Microwave heating times were determined by preparing mashed potato (105 or 205 g) according to instructions, placing them in cylindrical Pyrex glass containers to a height of 3 cm and covering them with a polypropylene lid. Mashed potato temperatures were measured at the geometric center, and at 1.0 and 3.5 cm from the center at the same depth (1.5 cm) on the same axis using fiber optic probes (FOT, FISO Technologies Inc., Quebec, Canada). The mashed potato was heated until all the probes reached 90°C and time required to reach 70, 72.2 or 73.8°C at the geometric center was calculated.

A 500 µL aliquot of the *Salmonella* spp. five serotype cocktail was added to 50 g of the prepared mashed potato to obtain an initial population of *ca*. 8.5 log CFU/g. The inoculated material (0.3 g) was placed in a fabric wick (3 cm length), placed inside non-inoculated mashed potato. Mashed potato in the container was placed at the center of the microwave carousel and heated for the selected times. Product temperature was determined as described above at the geometric center of the container. *Salmonella* spp. populations were enumerated by plating on selective and non-selective media.

RESULTS

The calculated heating times to achieve the target temperature of 70°C in the mashed potato at a 90% UCL were 128 s and 301 s for the small and large containers in

the low power microwave, respectively (Table 1). Heating in the low power oven in the large container produced a more uniform temperature distribution than the small container.

The calculated heating times for mashed potato placed in the small or large container were sufficient to eliminate *Salmonella* spp. (8.73 log CFU/g) when heated in the lower power microwave oven. The mean final internal temperature achieved was 72.7 ± 4.6°C and 79.3 ± 2.1°C for the small and large container, respectively. *Salmonella* spp. survival was observed in one (of three) mashed potato samples heated in the large container, with *Salmonella* spp. reductions of 2.93 log CFU/g observed in one sample. The internal temperatures achieved during heating in the high power oven were 71.9 ± 0.55°C and 69.1 ± 2.5°C for the small and large containers, respectively.

Table 1. Avg. heating times (min) of mashed potato to attain 70°C for various microwave power, container size and target end temperature with upper confidence limits.

Microwave power	Container size	Heating times (s)*		
		90%	95%	99%
Low (700 W)	Small	128	132	139
	Large	301	308	321
High (1,350 W)	Small	106	ND[@]	ND
	Large	151	152	153

* heating time for each Upper Confidence Limit; ND – Not determined

DISCUSSION

Survival of *Salmonella* spp. in the mashed potato could be attributed to several factors such the sample size and composition of the mashed potato (potatoes, margarine, milk, grated parmesan cheese and salt). Although Tassinari and Landgraf [2] used a larger container size than those used in this study, differences in heating times can be the main factor contributing to large differences in survival or destruction of the pathogen. Survival of *Salmonella* spp. even at temperatures considered lethal to the organism suggest non-uniform temperature distribution in the mashed potato.

CONCLUSION

Use of the high power microwave oven resulted in non-uniform heating of the product, and hence survival of *Salmonella* spp. Post-heating resting time should be provided to allow temperature equilibration and assure destruction of foodborne pathogens if present in the product.

REFERENCES

1. Scallan, E. R. M. Hoekstra, F. J. Angulo, R. V. Tauxe, Marc-Alain Widdowson, S. L. Roy, J. L. Jones, and P. M. Griffin. 2011. Foodborne illness acquired in the United States – Major pathogens. *Emerg. Infect. Dis.* 17:16-22.
2. Tassinari, A. D. R. and M. Landgraf. 1997. Effect of microwave heating on survival of *Salmonella* Typhimurium in artificially contaminated ready-to-eat foods. *J. Food Safety*. 17:239-248.

Optimization of Thickness of Microwaveable Multi-compartment Meals using Dielectric, Thermal, and Physical Properties

J. Chen, R. Lentz, P. Pesheck, A. Guru, D. Jones, and J. Subbiah

University of Nebraska-Lincoln, Lincoln, NE, USA

Keywords: wave-transmission matrix formulation method, reflection, transmission, electromagnetic wave propagation, microwaveable food product design.

INTRODUCTION

Non-uniform heating is the biggest challenge in cooking food products in domestic microwave ovens. Many analytical and numerical models have been developed to enhance understanding of microwave heating of foods, and serve as tools in later stage of food product development. The objective of this study is to present a simple model to describe the heating rate of a food product based on its dielectric, thermal, and physical properties, that will be helpful to assist food developers in the early design stage.

METHODOLOY

A simple 1-D model based on assuming an incident plane wave and uniform properties in two direction was developed to predict the average heating rate of a food product based on dielectric, thermal, and physical properties, as shown in Fig. 1. The power absorbed per unit volume of the dielectric food product at location z can be described as:

$$P(z) = \frac{1}{2}\omega\varepsilon_0\varepsilon''|E(z)|^2 \quad (1)$$

The total power absorbed by the food product with top surface area, A, and thickness, d, can be determined by:

$$Q = \int_{z=0}^{d} P(z)Adz = \frac{1}{2}\omega\varepsilon_0\varepsilon'' \int_{z=0}^{d}|E(z)|^2\, Adz \quad (2)$$

The average heating rate of the food product can then be calculated as:

$$\Delta T/\Delta t = Q/(\rho C_p Ad) \quad (3)$$

For a multi-compartment meal with two homogeneous food components placed in two compartments, each component thickness can be optimized to achieve the same average heating rate and therefore improved heating uniformity. The utility of the 1-D model to optimize the thickness of a multi-compartment meal based on dielectric,

thermal, and physical properties was validated by our previously validated 3-D multi-physics numerical microwave heating models. The effects of food component combinations, top surface area, food shape, and oven cavity on the utility of the 1-D model were comprehensively evaluated by simulating in the 3-D multi-physics numerical models considering each factor.

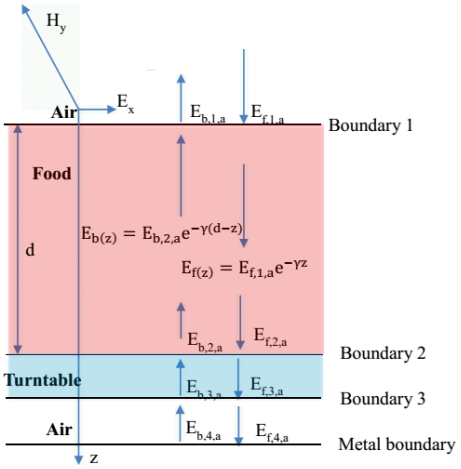

Figure 1. Schematic diagram of microwave transport in a food product. (E is the electric field; f indicates forward, b indicates backward, d is the thickness of food, z is the location, γ is the propagation constant).

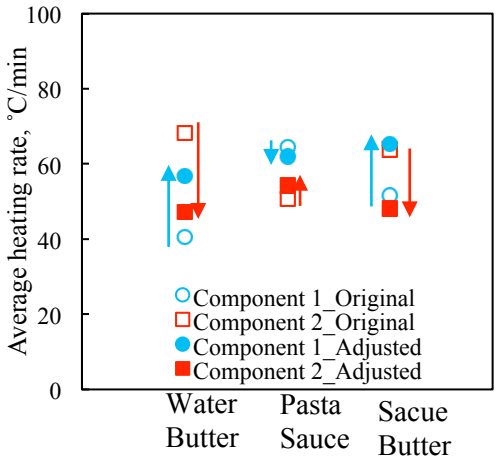

Figure 2. The effect of food component combination on the utility of using 1-D model to determine thicknesses of multi-compartment meals.

RESULTS AND DISCUSSION

Three different multi-compartment meals (water-butter; pasta-sauce; sauce-butter) were evaluated for the utility of the 1-D analytical model (Fig. 2). The average heating rate difference between two components were improved from 27.7 to 9.7 ˚C/min (decreased by 64.9%), 13.8 to 7.9 ˚C/min (decreased by 44.3%), and 12.2 to 17.1 ˚C/min (increased by 40.7%), respectively, for water-butter, pasta-sauce, and sauce-butter food systems. The bad performance of sauce-butter may be attributed to this specific food product combination cooked in this specific oven.

CONCLUSION

A simple 1-D model assuming microwave radiation normally incidents on the top surface of food product was developed to predict the average heating rate (average temperature) of a food product based on the dielectric, thermal, and physical properties. Based on the 1-D model, the thicknesses of two compartments of water and butter were adjusted from original equal thickness to achieve same heating rate. The meals with adjusted thicknesses showed improved average temperature and heating uniformity. This concept of optimizing thicknesses of a multi-compartment meal is valid for different oven cavities, food dimensions (top surface radius), food shapes, and food combination systems.

Microwave Browning of Foods: Recent Advancements in Improving Uniformity with a Novel Susceptor System

Mehrdad Mehdizadeh, Hank Chi, Ron Riegert, Nicole Blankenbeckler, and William Corcoran

DuPont Company, Wilmington, Delaware

Keywords: Microwave susceptors, microwave browning, microwave heating of foods

INTRODUCTION

In domestic microwave heating, disposable susceptors are used to direct a part of the microwave energy to provide intense heat to the surface of the food to create a crisping and browning effect [1]. The commercial susceptor aluminum layer, being so thin, acts as a resistive sheet of 200 Ω/Sq. This level of surface resistivity is proven to provide the optimum energy absorption for a typical microwave oven operating at 2450 MHz [2]. The utility of food susceptors is often limited by the microwave oven's inherent field non-uniformity. In locations where the electric field is either weak, or its main component is vertical to the plane of the susceptor, the crisping/browning is inadequate, which results in a soggy surface. We will introduce a field modification system that greatly enhance the uniformity and quality of crisping.

THE CONCEPT

Properly designed metallic objects, within a multimode cavity have the capability to shape and modify the fields to created desired heating effects. We have used a field director device [3], which working in conjunction with a conventional aluminum susceptor, greatly improves the uniformity and intensity of browning of the pizza crust microwave ovens with a turntable.

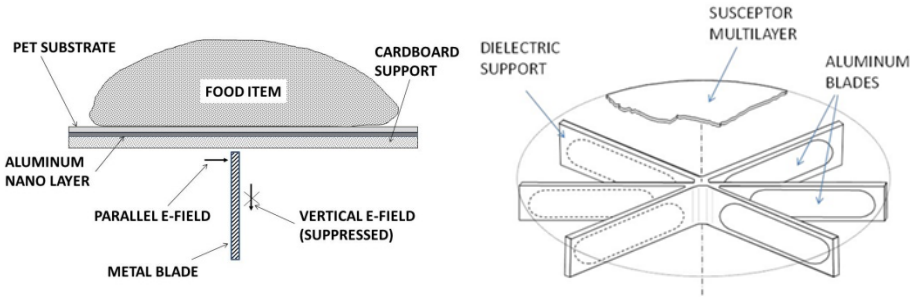

Fig. 1 The concept and practical implementation 6-lobed metal foil blade

In Fig. 1-a the metallic blade is placed vertical to the susceptor plane, on the opposite side where the food item is located. The presence of the blade encourages the electric field components parallel to the plane of the susceptor, at the expense of those vertical to the susceptor, which are not useful for activating the susceptor. In a situation where quasi-random electric fields are stirred with the aid of the microwave oven's built-in turntable, the overall impact of the metal blade is to enhance and make the browning of the surface of the food more even.

EXPEERIMENTS AND IMPLEMENTATION

The goal was to improve the browning uniformity of the crust for a pizza product with 18cm diameter where the built-in turntable for the microwave oven is used. Without the field modification device, there is a circularly symmetrical non uniform browning pattern that typically involves over- browning at the edges and sogginess at the center. Fig. 1-b shows the implementation of a six-lobed device that was made of 50 micron thick aluminum foil on cardboard backing. A folding mechanism was devised to create a flat structure to fit in a typical packaged food item.

To optimize the susceptor system design we used 3-D electromagnetic/thermodynamic COMSOL™ multi-physics modeling, as well as an experimental design to arrive at the desired dimensions for the susceptor system. The result is a robust system that lends itself to economically mass-produced disposable package.

REFERENCES

[1] Bohrer, T.H., et.al., Packaging techniques for microwaveable food, Handbook of Microwave Technology for Food Applications, Datta, K, et. al., editors, Marcel Dekker, New York, 2001

[2] Ceznek, J., et.al., Properties of thin metallic films for microwave susceptors, Czeck J. Food Sci. 21 (1), 2003 pp34-40

[3] US Patent 8,217,324

On the Use of Computer Simulation in the Design of Microwavable Food Packaging

F. Resurreccion[1], C. Crooks, V. Martinez, D. Pearson, and T. Brown

[1]Graphic Packaging International, Golden CO, USA

Keywords: Simulation, heating pattern, electromagnetic field distribution

INTRODUCTION

Several numerical methods are commonly used for solving coupled electromagnetic and heat transfer phenomena occurring during microwave heating of food. Among the popular are: Finite-Difference Time-Domain (FDTD), Finite Element Method (FEM), and Method of Moment (MoM). At Graphic Packaging International (GPI), the R&D group is utilizing FDTD method.

Since the first introduction of Finite-Difference Time Domain by Yee, in 1966 it became widely used in research area involving both analysis and design of devises and system that involves electromagnetic wave phenomena. Taflove is one the many researchers that picked up the concept of Yee and applied it extensively in the analysis of two and three-dimensional scattering problems (Taflove & Brodwin, 1975). FDTD method is favored over other methods that employ object discretization because of its computational efficiency and straightforward implementation of Maxwell's equation.

Using Quickwave 2014 simulation software, the R&D group of GPI is implementing FDTD primarily to design microwave active packaging. The active packaging is then imprinted in a microwavable paper based container (i.e. either in pressed or folding carton format) through chemical etching process depositing a thin layer of material representing the microwave active component.

The typical output of computer simulations useful in assessing the effectiveness of the microwave active component includes: (1) electromagnetic field distribution, (2) reflection coefficient, (3) heating pattern in a selected layer in food, and (3) temperature profile at a selected point in food. Depending on the location microwave active component, it will allow for field modification resulting in: (1) a relatively uniform heating pattern, and (2) prevention of runaway heating typically occurring at the edge of the food. This paper outlines the phases for implementing the computer simulation in designing the appropriate packaging for intended for a certain food system.

METHODOLOY

The method for using computer simulation in designing microwave active packaing was broken down into three (3) phases:

- Phase 1: determination of heating pattern in food using the desired geometry without the presence of active packaging.
- Phase 2: based from result of (1), strategically design the appropriate location of microwave active component in the package and re-run the computer simulation. Iteratively adjust the location of the microwave active component in the packaging until the desired heating pattern is obtained.
- Phase 3: Performance and abuse testing of the final packaging.

RESULTS

Illustrated below is a typical heating pattern output of phase 1 and phase 2 of the simulation process.

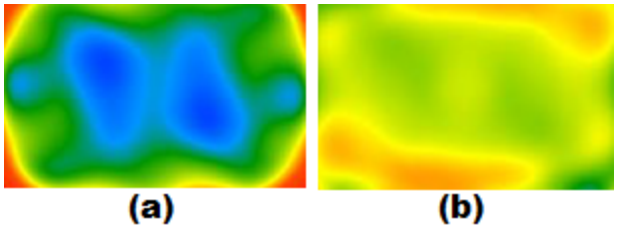

Figure 1. Simulated heating pattern (a) without active packaging and (b) with microwave active material

DISCUSSION

Upon incorporating microwave active material in the packaging, there was a marked improvement in the heating pattern of the food. The temperature of cold area at the middle portion (Figure 1a) increases (Figure 1b), as a result of field interaction with the microwave active material. Further, the visible hot spot at the four corners or the food (i.e. edge heating effect) in Figure 1a was mitigated in Figure 1b.

CONCLUSION

By following the method of computer simulation outlined in this paper and will be presented in details, an appropriate microwave active packaging for a certain food at a given geometry can be effectively designed.

REFERENCES

[1] K.S. Yee, Numerical solution of initial boundary value problems involving Maxwell's euqtions in isotropic media, *IEEE Transactions on Antennas and Propagation*, vol. 14, issue 3, pp.302-307, 1966.

[2] A. Taflove, and M.E. Brodwin, Numerical solution of steady-state electromagnetic scattering problems using the time-dependent Maxwell's equations, *IEEE Transactions on Microwave Theory and Techniques*, vol. 23, pp. 623-630, 1975.

[3] QWED, *QuickWave 2014 - Software for Electromagnetic Design*.

Analysis of Infrared Spectra of Microwave Heating Foods

Xiaojun Zhou[1], Xiaoyun Li[2], Min Liu[1], Wenbo Xiong1, Liang Pei[1] and Wenjie Fu[2]

[1]School of Opto-Electronic Information, University of Electronic Science &Technology of China, Chengdu, 610054, China
[2]School of Physical Electronics, University of Electronic Science &Technology of China, Chengdu, 610054,China

Keywords: infrared spectroscopy, microwave heating food, two-dimensional correlation spectrum, cluster analysis.

INTRODUCTION

Microwave ovens have been widely used world-wide because of their speed, energy conservation and convenience. However, there is some controversy about the safety of microwave heated food. Some suggest that microwave cooking is dangerous because the molecular structure of the food might be changed [1], and some consumers have even stopped using microwave cooking. But how different is the molecular structure of food prepared by microwave heating from traditional heating? To answer this question, in this paper infrared spectroscopy was used to analyze and compare microwave and traditionally heated food.

Infrared (IR) spectroscopy, which is advantageously rapid and non-destructive, has been used to analyze saturated and unsaturated fatty acids in edible oils [2], and to monitor fatty acid composition in virgin olive oil [3]. The infrared spectrum depends on molecular energy state transitions which reflect molecular condition. Therefore, the infrared spectrum can give molecular composition information about the heated food. In this paper, infrared spectroscopy, including two-dimensional correlation spectroscopy [4], was applied to analyze and compare microwave and traditionally heated oils.

EXPERIMENTS

Colza, corn, and peanut oils were microwave heated in a single mode cavity from room temperature (22°C) to 60°C, 80°C, 100°C, 120°C, 140°C, and 160°C separately. During the heating, the temperature of the food was monitored by an optical fiber temperature sensor. The IR spectra of the oils at different temperatures were obtained by a Spectrum Frontier Near/Mid FT-IR System (PerkinElmer Company U.S.). To compare with a traditional heating method, the infrared spectra were recorded from the same oils, heated to the same temperatures, using an electrically heated container.

The data of the original spectra were first analyzed by differential spectrum analysis; then two-dimensional (2D) correlation spectroscopy, principal component

IMPI'S 49th MICROWAVE POWER SYMPOSIUM San Diego, California, USA, June 2015

analysis and cluster analysis were used to analyze the molecular composition difference between foods heated by microwaves and traditionally. In the 2D correlation analysis, all parameters of the system were kept at the same value, except for the heating method. The measured spectra showed systematic variations that were processed with 2D correlation analysis for interpretation.

RESULTS AND DISCUSSION

Figure 1 shows the results of 2D correlation spectra of colza oil heated from room temperature to 160 °C. The top row is synchronous and the bottom row is asynchronous; the left column is a contour map representation and the right column is a fishnet representation of the 2D IR correlation spectrum. Both in synchronous and asynchronous spectra, the peak values of the microwave heated samples were smaller than electrically heated samples, but the peak locations of both samples were nearly the same.

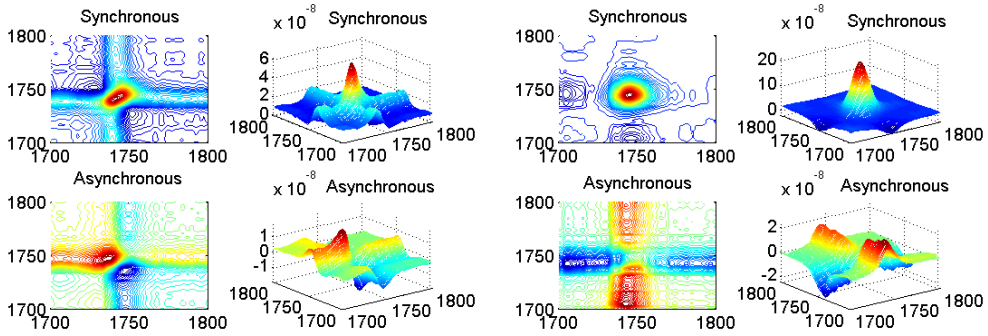

(a) microwave (b) electric

Figure 1. Two-dimensional correlation spectroscopy of colza oil after (a) microwave heating and (b) electrical heating

CONCLUSION

The results of the 2D IR correlation spectra and cluster analysis of the principal components in oils, after microwave and electrical heating, showed that their compositions were similar, but with slightly different proportions, which might be attributed to the shorter heating time using microwaves.

REFERENCES

[1] D. Schardt, Microwave Myths: Fact vs. Fiction. *Nutrition Action Healthletter*, April 10-12, 2005

[2] A. A. Christy, P. K. Egeberg, Quantitative determination of saturated and unsaturated fatty acids in edible oils by infrared spectroscopy and chemo metrics. *Chemometrics and Intelligent Laboratory Systems*, Vol.82, No.2: 130- 136, 2006.

[3] R. M. Maggio, T. S. Kaufman, M. D. Carlo, et al, Monitoring of fatty acid composition in virgin olive oil by Fourier transform infrared spectroscopy coupled with partial least squares, *Food Chemistry*, Vol.114, No.4: 1549- 1554, 2009.

[4] W. Choi, L.T. Nguyen, S.H. Lee, and S. Jun, Hybrid combination of microwave and ohmic heating technologies for multiphase foods, *Proc. 46th IMPI Microwave Power Symp., New Orleans, LA, June 2011*, pp. 62-67.

Dielectric Properties and Heating Rate of Broccoli Powder as Related to Radio Frequency Heating

Samet Ozturk[1], Fanbin Kong[1]

[1]Department of Food Science and Technology, University of Georgia, Athens, GA, USA

Keywords: Radio Frequency Broccoli Powder, Dielectric Properties, Heating Rate

INTRODUCTION

Many low moisture foods, including dried vegetables and spices, have been used for various applications such as coating materials, seasoning mixes and flavorings. Recently, an outbreak of *Salmonella Wandsworth and Typhimurium* has been associated with broccoli powder used for coating of snacks [3]. The safety issues of low moisture foods became a major concern in the food industry and forced it to seek an appropriate pasteurization process. Radio Frequency (RF) heating is a volumetric heating method with adjustable heating rate, appropriate energy efficiency, and short heating time. It has been applied in the food industry for applications such as disinfestation, enzyme inactivation, pasteurization and sterilization [1,2]. Because of its high potential, RF heating can be applied as an alternative pasteurization method for low moisture foods. The objectives of this study were (1) to measure the dielectric properties of the broccoli powder at frequencies from 1 to 30 MHz, different moisture contents (6.9-14.9% w.b.), and temperature from 20 to 80°C, (2) to evaluate the RF heating rate in broccoli powder as influenced by moisture content and compaction density at 27.12 MHz.

METHODOLOY

A precision LCR meter (4285A, Agilent Technologies, Palo Alto, CA) and liquid test fixture (16452, Agilent Technologies, Palo Alto, CA) were used to measure dielectiric properties of the broccoli powder as influenced by moisture content (% w.b.) temperature, and frequency (1 to 30 MHz). The RF heating rate in the broccoli powder was evaluated using a 27.12 MHz, 6kW RF oven (COMBI 6-S, Strayfield International, Wokingham, UK). The samples were placed in a small plastic bottle (height 4.8 cm, diameter 2.9 cm) between electrodes, and heated individually from 20 to 80 °C in the RF oven. The center temperature of the samples was recorded every 5 s using a data logger with a fiber optic sensor (Fiso Tech. Inc., Quebec, Canada). The distance between electrodes was fixed as 9 cm. The electric field penetration depth and the electrical conductivity of the broccoli powder were calculated following the procedures presented in [5] and [4], respectively.

RESULTS

The dielectric constant and loss factor of broccoli powder were directly proportional to both temperature and moisture content (6.9 -14.9% wet basis), but inversely correlated to the frequency at 1 to 30 MHz. The power penetration depth decreased with increase in temperature, frequency (Figure 1), and moisture content. The effective electrical conductivity of the broccoli powder increased with temperature and moisture content. The heating rate of broccoli powder at various moisture contents was in the range between 0.8 to 2.1 C°/s and highly correlated with dielectric loss factor, moisture content and compaction density. A linear relationship was found between compaction density and heating rate, and an exponential relationship was determined

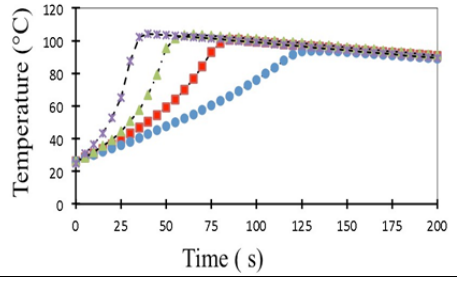

Figure 1. Typical temperature profile of the broccoli powder with different moisture content (6.9(•), 9.1 (■), 12.2(♦), and 14.9(★)% w.b.) at 27.12 MHz

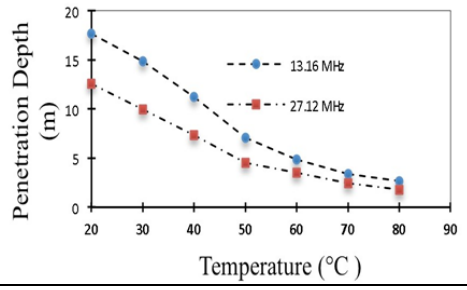

Figure 2. Penetration depth in the broccoli powder (moisture content 12.2% w.b.) for 13.56 and 27.12 MHz at temperatures from 20 to 80°C

DISCUSSION

The dielectric properties play an important role on the heating rate of the broccoli powder, which are influenced by moisture content, compact density, temperature and frequency. RF heating is much faster than the conventional heating process.

CONCLUSION

This study provides evidence that RF heating can be an effective method to pasteurize dried vegetables in short time and can potentially improve food quality.

REFERENCES

[1] Gao, M., Tang, J., Villa-Rojas, R., Wang, Y., Wang, S., 2011. Pasteurization process development for controlling Salmonella in in-shell almonds using radio frequency energy. Journal of Food Engineering 104 (2), 299–306.

[2] Manzocco, L., Anese, M., Nicoli, M.C., 2008. Radiofrequency inactivation of oxidative food enzymes in model systems and apple derivatives. *Food Research International* 41 (10), 1044–1049.

[3] Sotir, M.J., G. Ewald, A.C. Kimura, J.I. Higa, A. Sheth, S. Troppy, S. Meyer, R.M. Hoekstra, J. Austin, J. Archer, M. Spayne, E.R. Daly, and P.M. Griffin. 2009. Outbreak of Salmonella Wandsworth and Typhimurium infections in infants and toddlers traced to a commercial vegetable-coated snack food. *Pediatr. Infect. Dis. J.* 28(12):1041- 1046.

[4] Jiao Y, Tang J, Wang S, Koral T. 2014. Influence of dielectric properties on the heating rate in free-running oscillator radio frequency systems. *Journal of Food Engineering* 120(0):197-203.

[5] Wang Y, Tang J, Rasco B, Kong F, Wang S. 2008. Dielectric properties of salmon fillets as a function of temperature and composition. *Journal of Food Engineering* 87(2):236-46.

Effect of Radio Frequency Assisted Thermal Processing on Functional Properties of High Gel and Standard Egg White Powders

Sreenivasula Reddy Boreddy and **Jeyamkondan Subbiah**

University of Nebraska-Lincoln, NE, USA

Keywords: RF processing, foaming capacity, foam stability, gel firmness.

INTRODUCTION

Egg white powder (EWP) is an important ingredient in cakes, meringues (because of foaming ability) and in meat balls, sausage, surimi (because of gelling ability). Spray dried EWP is low in moisture, not sterile and may contain bacterial pathogens. Heat treatment modifies egg white proteins and improves the functional properties. At present, the EWP packed in 20 lb packages is pasteurized in hot rooms at 58–60°C for 10-15 days. The prolonged heat treatment increases the cost of energy. Microwave and radio frequency (RF) heating methods are known for rapid and volumetric heating of food products. The objective of this study was to determine the effect of RF assisted thermal processing on quality and functional properties of two major types of spray dried EWPs and to compare with the respective traditional hot room pasteurized EWPs.

METHODOLOY

Two types of spray dried EWPs of pH 7.0 (standard) and 9.5 (high-gel) were obtained from Henningsen Foods Inc., David City, NE, USA. The traditional hot room pasteurized EWPs of the same batch of samples were also procured after heat treatment for 14 days at 59°C and used for comparing its functional properties with that of RF pre-treated EWP. The RF assisted thermal treatment conditions were: RF heating to 60°C, 70°C, 80°C and 90°C followed by holding in a hot air oven at these temperatures for different periods ranging from 4 hours at 90°C to 72 hours at 60°C. The longer durations at each temperature were selected to improve the functional properties of EWP[1]. About 250 g of EWP was placed in a cylindrical polypropylene container and pre-heated to the desired temperature with a 6-kW parallel plate RF heating system (Fig. 1) operating at 27.12 MHz, then maintained at that temperature in a hot air oven for the desired period. The quality and functional properties of two EWPs investigated were color, foaming capacity (Fig.2), foam stability, solubility, water holding capacity (WHC) and gel-firmness (Fig.3).

RESULTS AND DISCUSSION

RF processing did not significantly affect EWP color and solubility, irrespective of the type and treatment conditions. In general, the foaming capacity, foam stability,

WHC and gel-firmness of RF pre-treated EWPs increased with an increase in temperature and treatment duration. The optimal treatment condition found for high-gel EWP were 90°C for ≥16 hours, which produced similar functional properties except lower (21%) foaming capacity (Fig.4). The optimal conditions for standard EWP were the same. An interesting aspect found in this study was that the gel strength of the standard EWP was significantly increased to that of high-gel EWP (Fig. 5). So far, the industry had an option for either high-foaming product or high-gelling product. We found that RF assisted thermal processing can increase the gelling strength of the high-foaming product without deteriorating foaming functionality. This can lead to newer applications of this functionally improved product.

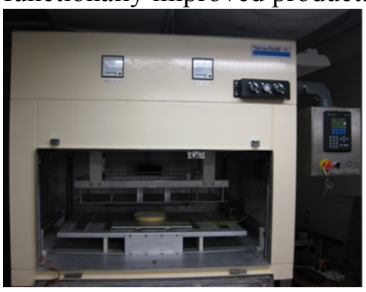

Figure 1. 6-kW RF heating unit

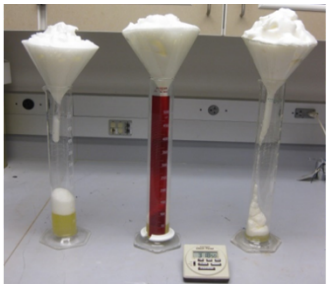

Figure 2. Foaming capacity

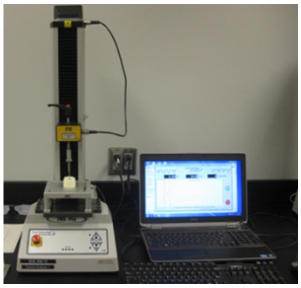

Figure 3. Gel-firmness

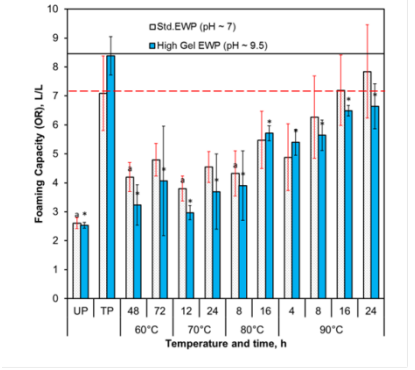

Figure 4. Foaming capacity (over run)

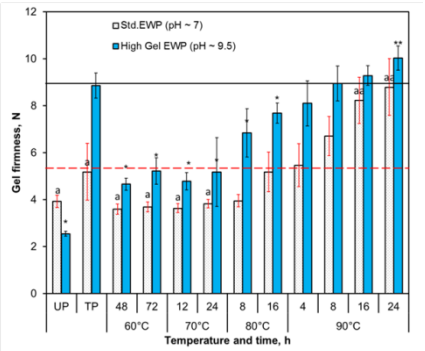

Figure 5. Gel firmness

(Note: UP: unpasteurized, TP: traditional hot room pasteurized; error bars represent +/- 1standard deviation, and asterisk '*' and letter 'a' indicate significant differences ($p < 0.05$) of high gel and std. EWPs, respectively with corresponding TP EWPs. '**' and 'aa' indicate significantly higher ($p < 0.05$) compared with corresponding TP EWPs.)

CONCLUSION

RF treatment can produce EWP with high foaming and gelling properties and reduce the pasteurization time to less than 1 day, while traditional thermal pasteurization takes 14 days.

REFERENCES

[1] Kato, A., H. R. Ibrahim, H. Watanabe, K. Honma, and K. Kobayashi, New approach to improve the gelling and surface functional properties of dried egg white by heating in dry state. J. Agric. Food Chem., vol. 37, no. 2, pp. 433-437, 1989.

Temperature and Moisture Dependent Dielectric Properties of Egg White Powder

Sreenivasula Reddy Boreddy and Jeyamkondan Subbiah

University of Nebraska-Lincoln, Lincoln, NE, USA

Keywords: Dielectric constant, Loss factor, Penetration depth.

INTRODUCTION

Knowledge of dielectric properties (DPs) such as dielectric constant (ε') and loss factor (ε'') of egg white powder (EWP) are needed in designing the continuous treatment systems employing radio and microwave (MW) frequencies, and in addressing the issues related to non-uniform heating. However, DPs data of EWP are not available in literature. DPs are influenced by many factors such as frequency, temperature, moisture content (MC) and density of food products[1]. The objectives of this study were to: 1) determine DPs of EWP in the frequency range of 10 to 3000 MHz, temperature range of 20°C to 100°C, and MC range of 5.5 to 13.4% d.b.; 2) develop polynomial regression models describing DPs of EWP as a function of temperature and MC at key radio (13.56, 27.12 and 40.68 MHz) and MW (915 and 2450 MHz) frequencies; and 3) determine the penetration depths of electromagnetic energy into EWP at frequencies of interest.

METHODOLOY

DPs of EWP in the MC range of 5.5-13.4% d.b. were measured with an impedance analyzer employing a coaxial probe technique in the frequency range from 10 to 3000 MHz and temperature range from 20°C to 100°C[2]. DPs data was analyzed at selected radio (13.56, 27.12 and 40.68 MHz) and MW (915 and 2450 MHz) frequencies as a function of MC and temperature and the polynomial regression models were fitted. The power penetration depths of EWP at five measured MC and temperatures were calculated from the average values of respective $\varepsilon'$and ε'' for five selected frequencies.

RESULTS

The ε' and ε'' increased with an increase in MC and temperature. Coefficients of fitted third-degree polynomial regression models for DPs are presented in table 1 and 2. Using the coefficients, the following third degree polynomial model for each frequency could be constructed and used to predict the ε' or ε'' in the experimental MC and temperature range.

$$\varepsilon_f' \text{ or } \varepsilon_f'' = a + bM + cT + dMT + eM^2 + gT^2 + hM^2T + iMT^2 + jM^3 + kT^3$$

where, ε'_f or ε''_f is dielectric constant or loss factor at a selected frequency f, respectively; a is an overall intercept; $b, c, d, e, g, h, i, j, and\ k$ are coefficients; M is moisture content, % d.b. (5.5≤M≤13.4); and T is temperature, °C (20 ≤T ≤100). As the temperature of the EWP at 8.0% d.b. MC increased from 20°C to 100°C, penetration depths varied from 1510 to 440 cm at RF (27.12 MHz) and from 142 to 11 cm at MW frequency (915 MHz). The MC and temperature dependent dielectric properties data of EWP obtained from this study provide opportunities for simulation studies that are needed to develop treatment protocols employing radio and MW frequencies.

Table 1 Coefficients of the third-degree polynomial regression model to predict the dielectric constant (ε') of egg white powder at five selected frequencies.

Terms in model	Coefficients at different frequencies				
	13.56 MHz	27.12 MHz	40.68 MHz	915 MHz	2450 MHz
a (intercept)	2.0349	1.0716	-1.0181	3.0271	1.3163
M	0.4634**	0.8001**	1.5031**	-0.3933**	0.1534**
T	-0.0829**	-7.732E-2**	-6.323E-2**	4.289E-3**	9.106E-3**
MT	3.341E-3**	2.774E-3**	5.29E-4**	-4.2E-4**	-8.0E-4**
M^2	-6.221E-2**	-0.1029**	-0.1820**	0.0424**	-1.326E-2**
T^2	1.32E-3	1.269E-3*	1.177E-3*	3.77E-4**	2.5E-4**
M^2T	1.3E-5	1.39E-4	3.47E-4*	1.29E-4*	9.8E-5
MT^2	4.517E-6	-5.08E-6	-1.0E-5	-4.94E-6	5.236E-7
M^3	2.637E-3	4.029E-3*	6.721E-3**	-1.4E-3	4.65E-4
T^3	-7.71E-6**	-7.15E-6**	-6.54E-6**	-2.54E-6**	-1.92E-6*

** and * model terms with the coefficients are significant at 0.0001 and 0.005 probability levels, respectively.

Table 2 Coefficients of the third-degree polynomial regression models to predict the loss factor (ε'') of egg white powder at five selected frequencies.

Terms in model	Coefficients at different frequencies				
	13.56 MHz	27.12 MHz	40.68 MHz	915 MHz	2450 MHz
a (intercept)	-1.1144	1.0032	3.4406	-0.5758	-0.209
M	0.4617**	-0.2676**	-1.0913**	0.1674**	7.514E-2**
T	2.851E-3**	-1.042E-2**	-2.505E-2**	7.501E-3**	1.346E-3**
MT	-1.117E-2**	-5.75E-3**	-3.7E-4**	-1.32E-3**	-1.8E-4**
M^2	-3.171E-2**	4.137E-2**	0.1239	-1.691E-2**	-7.23E-3**
T^2	6.99E-4	5.67E-4*	4.34E-4*	1.68E-4**	1.21E-4**
M^2T	7.17E-4**	3.8E-4**	5.2E-5	1.15E-4**	4.8E-5*
MT^2	2.1E-5*	2.2E-5**	2.4E-5*	-7.45E-8	-1.6E-6
M^3	3.31E-4	-1.89E-3	-4.43E-3*	5.3E-4	2.15E-4
T^3	-4.66E-6**	-3.93E-6**	-3.23E-6*	-1.17E-6**	-7.79E-7**

CONCLUSION

The polynomial models found to describe the variation of the dielectric properties of EWP within the experimental range of moisture content and temperature with R^2 values ≥0.957 and with RMSE≤ 0.171.

REFERENCES

[1] S.O. Nelson, Dielectric properties of grain and seed in the 1 to 50 MHz range. Transactions of the ASAE, vol.8, no. 1, pp.38–48, 1965.

[2] Guo, W., Tiwari, G., Tang, J., & Wang, S. (2008). Frequency, moisture and temperature dependent dielectric porperties of chickpea flour. Biosystems Engineering, 101(2), 217-224.

Thermodynamic Modeling of Orange Peel Dried by Hot Air-Microwave

Clara Talens[1], Marta Castro-Giráldez[2], Pedro J. Fito[2]

[1]AZTI-Food Research, Parque Tecnológico de Bizkaia, Derio, Spain
[2] Laboratorio de Propiedades Dieléctricas, Instituto Universitario de Ingeniería de Alimentos para el Desarrollo, IIAD, Universidad Politécnica de Valencia, Spain

Keywords: orange peel, microwave, drying, thermodynamics, dielectrics, microstructure.

INTRODUCTION

Dielectric properties are necessary to quantify the overall heating produced when any food product is exposed to microwave energy. The aim of this work was to develop a thermodynamic-electric model for understanding internal heating, water transport mechanisms, drying kinetics and microstructure changes occurring during hot-air microwave drying of orange peels.

METHODOLOGY

Orange peel samples were dried with a specially designed hot air-microwave drying oven (HAD + MW) at 55ºC combined with different MW powers. Samples were removed at different times over 120 min. Dielectric properties were measured with an Agilent 85070E open-ended coaxial probe connected to an Agilent E8362B Vector Network Analyzer.

RESULTS

The total distribution of energy was calculated as $E_T = E_{HAD} + E_{MW}$; where E_{HAD} is the energy supplied by the hot air and E_{MW} is the energy supplied by microwaves. The microwave energy absorbed and transformed into heat energy was calculated as $E_{MW} = E_{abs} \cdot r_{MW}$; where E_{abs} is the overall energy absorbed and $r_{MW} = \frac{\varepsilon''}{\varepsilon' + \varepsilon''}$, is the microwave energy dissipation ratio (Figure 1c).

In Figure 1a it was possible to observe in a psychometric chart the beginning of drying at the initial value of the water activity ($a_w^0 \approx 0.97$) and finishing at the line of drying conditions. Samples treated by HAD + MW showed high levels of enthalpy at the beginning of the treatments, when high water activity produces higher dissipation of microwave energy. In order to estimate the surface temperature, an iteration system was developed as shown in Figure 1d and temperature evolution was plotted in Figure 1b.

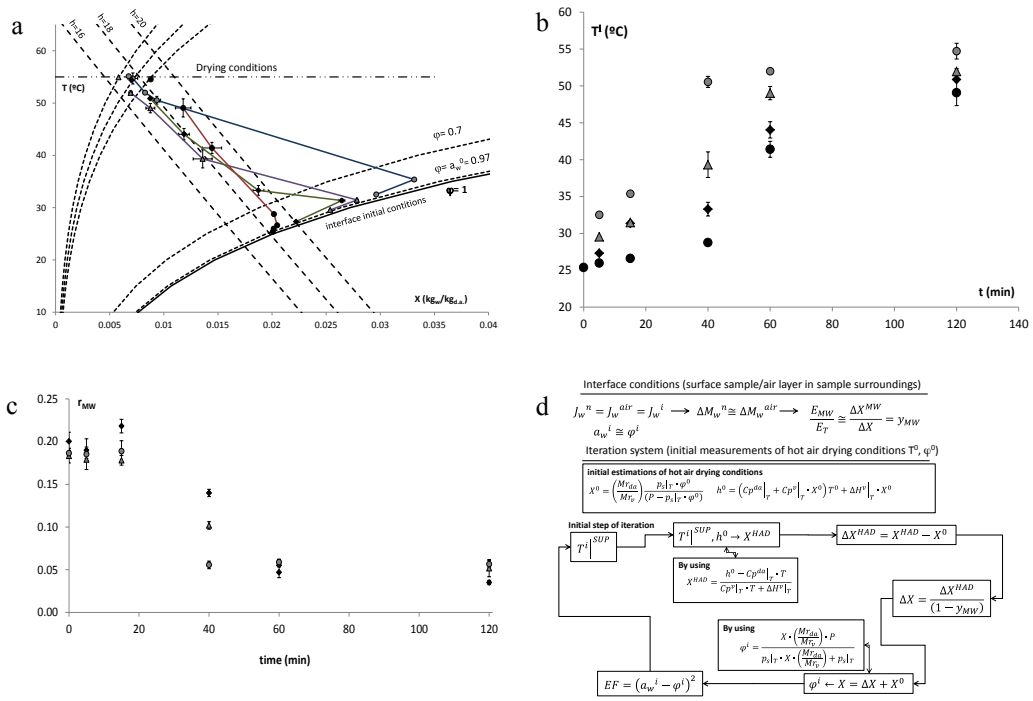

Figure 1. ● HAD, ◆ HAD+2 W/g, ▲ HAD+4 W/g, ● HAD+6 W/g; 1a (Evolution of interface air conditions throughout the drying process); 1b (Interface temperature evolution); 1c (MW energy dissipation ratio (r_{MW}); d (Iteration scheme).

DISCUSSION

In samples treated by HAD+MW, the mechanisms of surface evaporation and microwave dissipation by penetration were coupled. The result of coupled behaviors produces internal evaporation and therefore induces an internal swelling (volumetric sample expansion). Depending on the predominant mechanisms (HAD shrinkage and MW swelling) samples suffer volumetric expansions or contractions. HAD+MW treatment reduced drying time changing the structural properties and reducing the energy expended.

CONCLUSION

This model allows optimizing the traditional hot air drying by coupling microwaves as a novel time-efficient process for citrus by-products valorization.

REFERENCES

[1] M. C. Garau, S. Simal, C. Rosselló and A. Femenia, Effect of air-drying temperature on physico-chemical properties of dietary fibre and antioxidant capacity of orange (Citrus aurantium v. Canoneta) by-products. *Food Chem., 2007*, *104*, pp. 1014-1024.

[2] H. Feng, Y. Yin and J. Tang, Microwave Drying of Food and Agricultural Materials: Basics and Heat and Mass Transfer Modeling. *Food Engineering Reviews, 2012*, *4*, pp.89-106.

Effect of Frequency of Updating Dielectric Properties on Accuracy and Computation Time of a Microwave Heat-Mass Transfer Model

J. Chen, K. Pitchai, S. Birla, D. Jones, M. Negahban, and J. Subbiah

University of Nebraska-Lincoln, Lincoln, USA

Keywords: microwave heating, heat transfer, mass transfer, finite element analysis, rotation, updating dielectric properties.

INTRODUCTION

A comprehensive three-dimensional finite element simulation for describing microwave heating of a food product on a rotating turntable is computationally intensive and time consuming [1]. To model the microwave heating of food rotating on a turntable, reduce the computation, and capture the variation of properties with time, normally, discrete rotational steps are used in simulating microwave heating of food products when they are on a turntable, and, typically, dielectric properties are updated at every rotational step. Liu et al. [2] used this typical approach for evaluating the microwave heating of rotating fresh mashed potato and found that the dielectric properties need not to be updated frequently if the penetration depth does not change considerably with temperature change. However, the dielectric properties and penetration depth change considerably with temperature for a frozen food product especially during phase change. Therefore, it is necessary to determine the necessary frequency of updating the dielectric properties during microwave heating.

METHODOLOY

In this study, we evaluate a simplified approach in which the frequency of updating dielectric properties was reduced from once every rotational step to once every rotational cycle, and the heat source was averaged from all the rotational steps in one rotational cycle for heat and mass transfer analysis. The models using typical and simplified approaches were developed and validated for heating of a 550 g tray of frozen mashed potato for 6 minutes in a 1250 W microwave oven on a rotating turntable. The spatial variation of the top surface temperatures of the mashed potato was acquired by an infrared camera, the transient temperatures at six locations was recorded by fiber optic sensors, and the total moisture loss during heating was measured.

Table 1. Comparison of physics analysis and computation time between two updating approaches

Approaches	Number of EM field analysis	Number of heat and mass transfer analysis	Total computation time, h
Updating at each rotational step (Typical)	432	432	550
Updating at each rotational cycle (Simplified)	432	36	96

RESULTS AND DISCUSSION

Both approaches of updating dielectric properties showed similar spatial and point temperature, as well as moisture predictions, which also matched well with the experimental validation. However, the two approaches required different computation time, as shown in Table 1.

The two approaches needed the same time for the EM field analysis. However, different computation times were needed for the heat and mass transfer analysis, although the total heating time was the same for two approaches (6 min). In this study, the implicit method was used ("free time step") in the time-dependent solver for the coupled heat and mass transfer analysis, where the solver can choose time steps according to the total heating time settings at that step (10 s for one rotational cycle in the simplified approach versus 0.83 s for each rotational step in the typical approach) and convergence performance. The solver typically starts with a smaller time step. Based on convergence, the solver then starts using larger and larger time steps during the remaining part of the heating. In case of short heating steps of 0.83 s, the solver restarts more frequently (432 times) and takes a longer time than solving a relatively longer heating time (10 s) using with less frequency (36 times). Therefore, the simplified approach of updating at each rotational cycle used less computation time (96 h) than the typical approach of updating at each rotational step (550 h).

CONCLUSION

The experimental spatial variations of temperatures on the top layer of the mashed potato at 2, 4, and 6 min of heating, the transient temperatures at six locations, and the total moisture loss showed good agreement with the predicted results. While the simulations using both approaches showed good agreement with the experiments, the simplified (less-frequent updating only at each rotational cycle) approach reduced the computation time by 83%.

REFERENCES

[1] J. Chen, K. Pitchai, S. Birla, M. Negahban, D. Jones, and J. Subbiah, Heat and mass transport during microwave heating of mashed potato in domestic oven – model development, validation, and sensitivity analysis. *J. Food Sci*. vol.79, pp.1991–2004, 2014.

[2] S. Liu, M. Fukuoka, N. Sakai, A finite element model for simulating temperature distributions in rotating food during microwave heating. *J. Food Eng*. vol. 115, pp. 49–62. 2013.

Plant Growth and Yield of Wheat and Canola in Microwave Treated Soil

Graham Brodie, Natalie Bootes, and George Reid

University of Melbourne, Dookie, Australia

Keywords: Microwave soil treatment, crop growth, crop yield.

INTRODUCTION

Chemical soil fumigation is commonly practiced in some agricultural industries [1]. Several fumigant chemicals, including methyl bromide and metham sodium, have serious health and environmental concerns, and are being systematically removed from the market.

A sustained research program has demonstrated that microwave treatment of *in-situ* soil, using a horn antenna applicator, can effectively kill weed plants and their seeds [2]. Microwave soil treatment can also reduce populations of some organisms in the soil, such bacteria and nematodes [3], without significantly affecting fungi and protozoa; however the effect of microwave soil treatment on subsequent crop growth has not been well studied. This paper presents an experimental assessment of plant growth and yield for two winter crop species grown in microwave treated soil.

METHODOLOY

Forty pots (15 cm diameter by 20 cm deep) of top soil, harvested from a regularly cropped paddock at Dookie agricultural campus of the University of Melbourne, were randomly subjected to varying amounts of microwave energy [0 (control), 168, 384, and 576 J cm^{-2}], applied using a horn antenna with aperture dimensions of 110 mm by 55 mm, fed from a 2 kW, 2.45 GHz microwave generator. The microwave treatments caused a mean temperature rise in the top 2 – 3 cm of soil by 18 °C, 44 °C, and 70 °C, respectively.

After cooling over night, half of these pots were planted with ten seeds per pot of wheat (*Triticum spp.*) and half were planted with ten seeds per pot of canola (*Brassica napus*) to achieve 5 replicates of each microwave treatment combination for each species. The pots were placed in a glass house and watered three times per week. After the plants were well established the pots were thinned to three plants per pot. Growth and final seed yield were assessed.

RESULTS

Plant maturation rate, mean plant height (Figure 1), and mean yield per pot (Table 1) all increased significantly as the level of applied microwave energy increased.

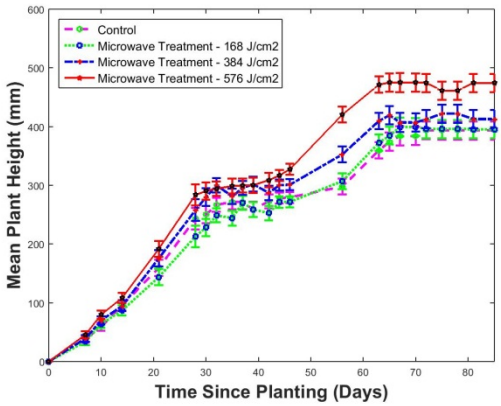

Figure 1. Mean wheat plant height as a function of time since planting and microwave soil treatment energy (error bars represent LSD for P = 0.05).

Table 1. Mean yield (grams per pot), 85 days after planting, as a function of applied microwave treatment energy

Applied Microwave Energy ($J\ cm^{-2}$)	0	168	384	576	LSD (P = 0.05)
Wheat Grain	0.66^a	0.68^a	0.75^a	1.25^b	0.30
Canola Pods	0.30^a	0.36^a	1.25^b	1.95^c	0.55

Note: entries with different superscripts across the rows are statistically different from one another

DISCUSSION

Mean wheat grain yield per pot, for the highest microwave treatment, was 189 % higher than the mean grain yield for the control treatment and mean canola pod yield per pot, for the highest microwave treatment, was 650 % higher than the control (Table 1).

CONCLUSION

Microwave soil treatment significantly improve crop growth and yield in a pot trial. Microwave energy may be a viable alternative to chemical soil fumigation in agricultural systems; however a thorough economic analysis is yet to be completed.

REFERENCES

[1] S. A. Fennimore, M. J. Haar and H. A. Ajwa, Weed Control in Strawberry Provided by Shank- and Drip-applied Methyl Bromide Alternative Fumigants, *HortScience,* vol. 38, no 1, pp. 55-61, February 1, 2003 2003.

[2] G. Brodie, C. Ryan and C. Lancaster, Microwave technologies as part of an integrated weed management strategy: A Review, *International Journal of Agronomy,* vol. 2012, pp. 1-14, 2012.

[3] G. S. Rahi and J. R. Rich, Potential of microwaves to control plant-parasitic nematodes in soil, *Journal of Microwave Power & Electromagnetic Energy,* vol. 42, no 1, pp. 5-42112, 2008.

Microwave Induced Thermal Gradients in Multiphase Systems

Alvin Kennedy[1]*, Arron Reznik[2], Solomon Tadesse[1]

[1]Department. of Chemistry, Morgan State University, Baltimore, MD, USA
[2]Department of Mathematics, Morgan State University, Baltimore, MD, USA

Keywords: microwave heating, immiscible liquids, inversion, mixture, mathematical model, MITG, multiphase.

INTRODUCTION

Microwave induced thermal gradients (MITG) occur in heterogeneous systems composed of polar and non-polar phases. The selective microwave irradiation of polar components in heterogeneous multiphase systems, and the resulting heat transfer to non-polar components of those systems, is not well understood. This process is of significant importance in medical, biological, chemical, and other multiphase systems. Kennedy et al [1], [2] first reported MITG for several polar and non-polar immiscible biphase systems of varying densities. It was observed that when the polar phase was denser than the non-polar, heat transfer via conduction, produced large (> 100 ^{0}K) sustainable temperature differences between the two phases. For biphase systems, in which the polar phase was denser than the non-polar phase, convection was the dominate factor and produced a persistent MITG (> 20 ^{0}K). In this presentation, we report that molecular structure and chemical composition of the biphase system is important in maintaining immiscibility after a MITG is produced.

METHODOLOGY

Temperature was measured as a function of time for the chemical components of biphase immiscible fluid systems during heating in a modified CEM Microwave Sample Preparation System MDS-2000 oven (power 630 W, frequency 2450 MHz). A Teflon-perfluoroalkozy (with wall thickness of 0.047 cm) microwave sample vessel, with a modified cover was equipped to accommodate several thermowells at varying depths, in addition to a pressure tube and pressure sensitive cap. All experiments were conducted under constant volume conditions at 30% power, maximum temperature 450 °K, maximum pressure 1380 kN/m², and run time of 10 min.

RESULTS

Biphase fluid systems consisted of water (denser polar phase) and several non-polar hydrocarbons (less dense upper phase). The results of the temperature measurements are shown in Figure 1 for samples consisting of 30 ml of each fluid.

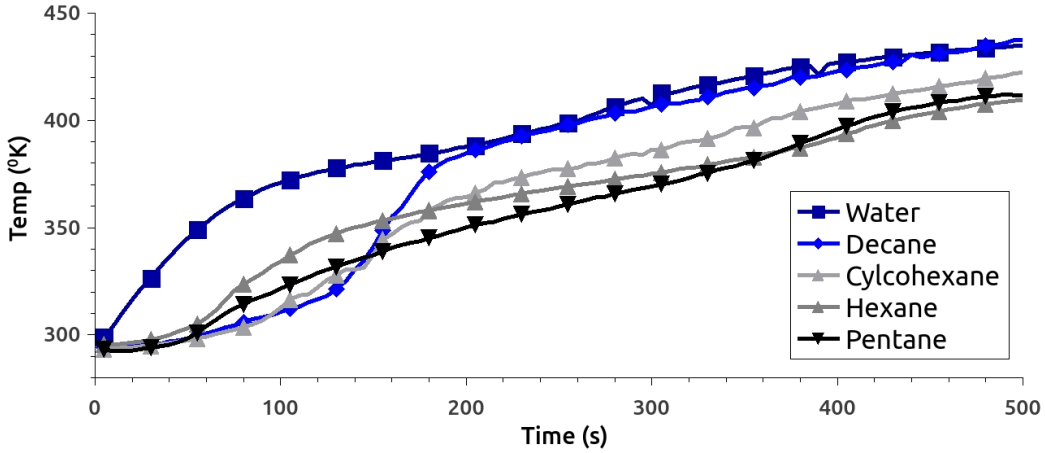

Figure 1. Microwave heating of biphase water/alkane systems.

DISCUSSION

MITG was observed for all biphase fluid water/alkane systems in the first 110 seconds. The average temperature of the water phase was represented by the blue line for all experiments. The largest temperature difference was in the water/decane system at 60K at 110 seconds. Water/hexane and water/pentane had the smallest difference in the same region of 39 K and 50 K respectively. The water/decane systems is miscible after 180 s, which agrees with Wachtor *et. al* that microwave heated biphase systems can become miscible [3]. The remaining biphase systems water/cyclohexane, water/pentane and water/hexane had MITG differences of 11K, 22K and 25K, respectively.

CONCLUSION

The results of these and other experiments demonstrated that the MITG is dependent on molecular structure and chemical composition of the multiphase systems.

REFERENCES

[1] Kennedy A., Reznik A., Tadesse S., Nunes J., Time dependence of component temperatures in microwave heated immiscible liquid mixtures, *Journal of Microwave Power and Electromagnetic Energy,* **42**(3), 52 - 64 (2009)

[2] Kennedy A., Reznik A., Tadesse S., Nunes J., Time dependence of component temperatures in microwave heated immiscible liquid mixtures, *Journal of Microwave Power and Electromagnetic Energy,* **45**(1), 5-14 (2011)

[3] Wachtor AJ, Mocko V, Williams DJ, Goertz MP, Jebrail FF., Jour*nal of Microwave Power and Electromagnetic Energy,***47** (3), 210-223 (2013)

Dynamic Analysis of Continuous Flow Processing of Biodiesel Production and Heating Uniformity Improvement

H.Zhu and K. Huang

Sichuan University, Chengdu, China

Keywords: Microwave, continuous process, biodiesel, multiphysics modeling

INTRODUCTION

Microwave assisted biodiesel production is a complex interplay of electromagnetics, reaction between different components and heat & mass transfer in a tube for continuous manufacturing. A comprehensive physics-based model is developed to understand and optimize the microwave processing of continuous production of biodiesel.

METHODOLOY

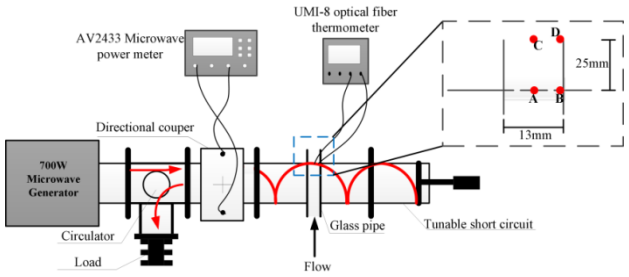

Figure 1. Experiment system for microwave continuous producing of biodiesel

In Fig.1, shows the experimental system developed to validate the multiphysics model. The microwave generator (2450 MHz) power was 700W. Volume ratio of methanol to acid of 1:1 was employed, and the mass fraction of catalyst (concentrated sulfuric acid) to the whole reaction solution was 1%. The solution flows into the tube from the bottom, four different velocities were employed. They being 10, 8, 6 and 4cm/s.

RESULTS

The measured and computed temperatures of site A and B was camparised in table.1. Excellent agreement was found between experimental values and model predictions with a maximum relative error of 0.908%.

It's obvious that the 4cm/s velocity is better for the process, due to the more uniformity of the temperature distribution. But some non-uniformity still exists inside for higher velocity. Here, the distributions of power loss, velocity and temperature arise along the line which crossed site A and B were plotted in Fig.2. It's shown that even

though the power loss is higher near the center, the temperature rise is not as much as it is near the wall. This is due to heat energy being converted away because of much higher velocities near the center.

Table 1. The averaged computed and measured temperature results at the A and B sites under different velocity.

Velocity	Site	Computational Temperature (*K*)	Measurement Temperature (*K*)	Error (%)
4	A	340.86	338.35	0.736%
	B	340.40	340.20	0.059%
6	A	330.96	329.80	0.350%
	B	339.17	338.35	0.237%
8	A	324.14	325.25	0.342%
	B	337.99	336.90	0.322%
10	A	320.06	321.70	0.512%
	B	338.17	335.10	0.908%

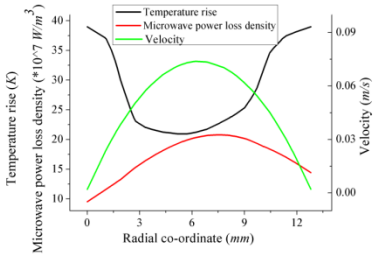

Figure 2. The axial velocity profile, temperature rise profile and electromagnetic power loss density profile along the line which crossed site A and B

Based on the the validated model, the inside structure of the tube was optimazied. In Fig.3a, the cross-sectional temperature profiles at the top of the optimazied tube were plotted, Fig. 3b is the profiles for the tube without stureture inside and Fig. 3c is the structure schematic of the new tube. The results indicated that much more heating uniformity can be obtained by the new optimized tube.

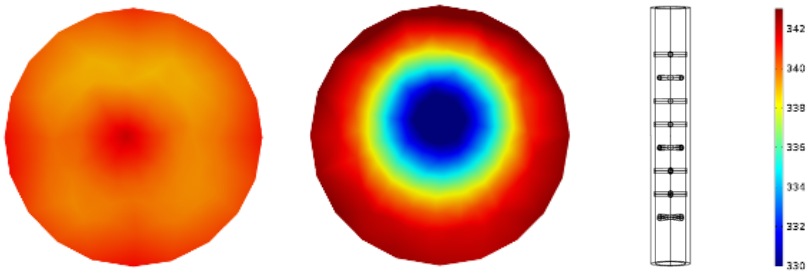

(a) (b) (c)

Figure 3. 2D temperature profile at the top of the tube, (a) with structure inside the tube, (b) without structure in the tube, (c) the structure schematic of the tube (Unit: *K*)

CONCLUSION

The model developed is elaborate from the point of view of physics can explain the process of microwave-assisted production of biodiesel. Excellent computed results obtained and the tube was optimazied to improve the heating uniformity for biodiesel reaction solution. The modeling is useful for optimize the process before scaling up.

Molecular Orbital Verification of Microwave-Driven Chemistry: Synthesis of Fluorescein without Solvent and Catalyst

Takeko MATSUMURA [1], Shozo YANAGIDA [2]
[1] Minerva Light Laboratory, L.L.C. Soraku/Kyoto, Japan
[2] Osaka University, Suita, Japan

Keywords: fluorecein, density functiona theory, molecular mechanics, Milliken charge

INTRODUCTION

MW-driven synthesis is characterized by a high reaction rate and selectivity to target molecules. We found that fluorescein can be synthesized by solvent and acid catalyst-free MW-driven thermal reactions[1)] The so-called MW thermal catalysis predicts that resorcinol and phthalic anhydride aggregates in the stationary state via hydrogen bonds and van der Waals and Coulomb interactions (vdW&Clb), and the molecularly integrated aggregates bring about large dielectric medium, being activated thermally under MW irradiation. The solvent/catalyst-free formation of fluorescein is verified by computational molecular orbital analysis.

METHODOLOY

DFT (B3LYP, 6-31G(d) basis set with Spartan'14 (Wavefunction, Inc. Irvine, CA) simulated the molecular self-aggregates that were non-covalently bonded via vdW&Clb.

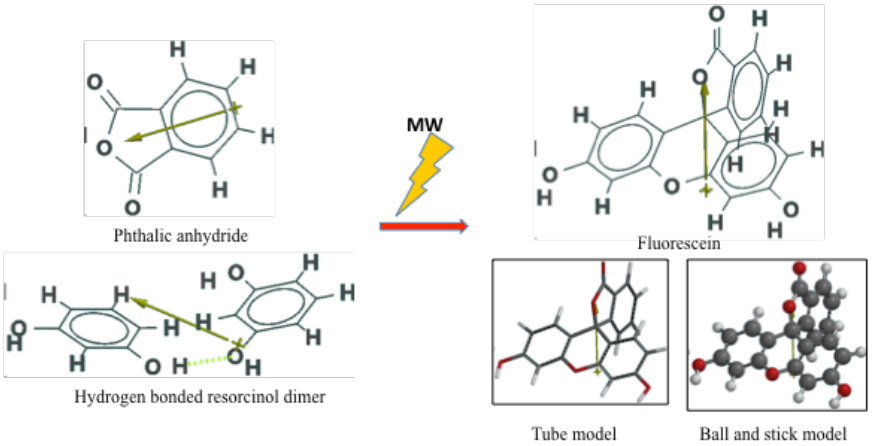

Figure 1. Reaction scheme of solvent-free and acid catalyst-free formation of fluorescein from phthalic anhydride and hydrogen-bonded resorcinol dimer

The self-association of resorcinol via a hydrogen bond and its association with phthalic anhydride via vdW&Clb were optimized by molecular mechanics (MMFF in Spartan) and simulated by DFT to equilibrium state of the association [1].

RESULTS AND DISCUSSIONS

Phthalic anhydride (10g) and resorcinol (15g) were place in a beaker and irradiated with MW(700W). The powdered mixture started to melt in 2 minutes and became red-orange in 5 minutes (Figure 1). The aggregation of the hydrogen bonded resorcinol dimer with phthalic anhydride are optimized by MMFF, and DFT simulation give the equilibrium states of molecular integrated models, 1, 2 and 3 in Table 1 (with slightly different parameters).

Table 1 The MMFF/DFT-simulated models for aggregation of resorcinol and phthalic anhydride

Simulated model	E (kcal/mol)	ΔE (kcal/mol)	LUMO (eV)	HOMO (eV)	Dipole (debye)
Model 1	-814716.48	-10.64	-2.37	-5.57	3.82
Model 2	-814719.59	-13.75	-2.81	-5.56	4.62
Model 3	-814725.02	-19.18	-3	-5.7	4.71

The formation energy (ΔE) suggests that the aggregations were exothermic. The dipole becomes larger than the starting molecules. Figure 2 shows details of the MMFF/DFT-simulated molecular orbital structure (HOMO, solid, LUMO, net) of the model The Mulliken charge and the proximity of the carbon atoms in the range of the van der Waals distance explain the simultaneous spiro-bonding by MW thermal catalysis, i.e., MW-induced activation by dielectric loss of molecular integrated dipole systems.

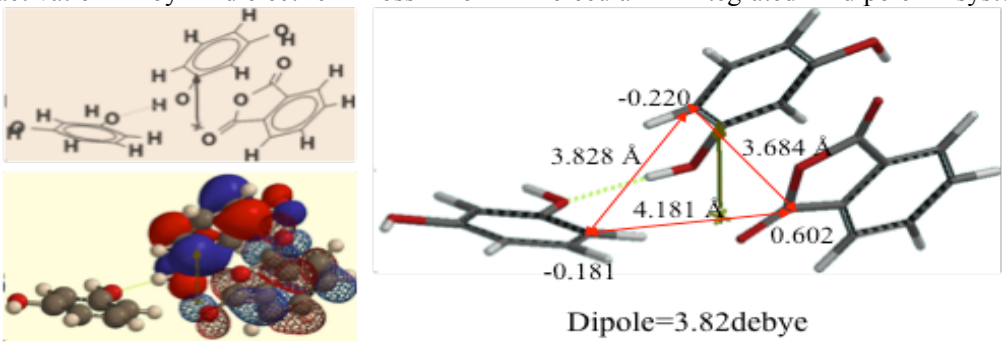

Figure 2. The molecularly integrated structure of phthalic anhydride and hydrogen-bonded resorcinol dimer (Model 1) DE=-10.64kcal/mol

CONCLUSION

MW-driven reactions should be verified by molecular orbitals of non-covalent reagent systems formed via vdW&Clb for optimization of MW-thermal catalysis.

REFERENCES

[1] Hehre. W. J. Application of Graphical models in Book, A Guide to Molecular Mechanics and Quantum Chemical Calculatio, Chapter 19, 473, Wavefunction, Inc. 2003.

Aurora Observation in Microwave Oven and Molecular Modeling

Shozo Yanagida[1, 2], Toshiyuki Kida[1)] and Takeko Matsumura[2]
[1] Osaka University, Suita, Japan
[2] Minerva Light Laboratory, L.L.C. Soraku/Kyoto, Japan

Keywords: nitrogen-water complexes, computational chemistry, van der Waals and Coulombic interactions, density functional theory

INTRODUCTION

Microwave (MW) radiation energizes electrons in vapor when solid materials in a MW oven reach high temperature. The energized electron initiates plasma phenomena, and plasma-state N_2 gas emits violet to pale lavender blue and more pink light [1]. The Aurora is a natural plasma phenomena with atmospheric constituents, caused by energized electrons from the sun. We observed aurora when a vacuum-sealed Pyrex glass tube was irradiated in a MW oven. Computational molecular modeling was used to verify and interpret chemical phenomena by designing given molecules [2]. We defined some van der Waals complexes of N_2 with H_2O, and calculated molecular orbitals and UV/Vis absorption spectra of the defined complexes. The radical anions and cations from them were defined as plasma-state molecules and their UV/Vis absorption spectra were calculated and analyzed.

METHODOLOY

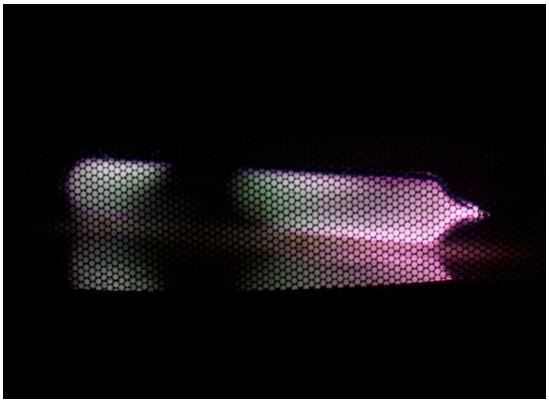

A Pyrex glass tube (ϕ=20) was filled with 10^{-3} atmospheric air and sealed in the presence of carbon nanotubes as an electron emitting source under MW irradiance. Another Pyrex tube was sealed under vacuum without carbon nanotubes. The former emitted bright white light, while the latter emitted blue, green, and pink light as seen in the photo. Molecular modeling was conducted using density functional theory (DFT)(B3LYP, 6-31G* of Spartan'14 [2].

RESULTS AND DISCUSSIONS

N_2 and H_2O molecules were desorbed from the Pyrex tubes during MW heating, and are suspected as being essential in changing the emission from white to colorful. We defined molecular models of $N_2\&(H_2O)_n$ (n=1~3) as emissive molecules and the radical cations, $[N_2\&(H_2O)_n]^+$ and the radical anions, $[N_2\&(H_2O)_n]^-$ as plasma-state molecules. Water cluster $(H_2O)_n$ (n=2, 3), their cation radicals, $[(H_2O)_n$ (n=2, 3)$]^+$ and the radical anions $[(H_2O)_n$ (n=2, 3)$]^-$ are also calculated as essential molecules in the aurora.

Nitrogen molecules form charge transfer complexes with H_2O and $(H_2O)_3$, and some radical anions and cations are verified to form via van der Waals and Coulombic interactions, and the UV/Vis absorption spectra, the formation energy and molecular orbital structures were calculated (Table 1). $N_2\&H_2O$ and $N_2\&(H_2O)_3$ absorb in the UV at longer wave length than those of H_20 and $(H_20)_3$, and all of the simulated radical anions and cations were calculated to be largely endothermic. The calculated UV/Vis absorption spectra give relatively large intensity (f) value, suggesting that the plasma-state molecules filter emission from the white nitrogen discharge emission light. Figure 1 illustrates that while $N_2\&(H_2O)_3$ is calculated to absorbs only UV light as a charge transfer complex via HOMO-LUMO interaction, the plasma-state $[N_2\&H_2O]_3]^-$ is calculated to absorbs red light (λmax=617nm(f=0.0017)). The green aurora may be explained as due to selective red light absorption by the plasma-state $[N_2\&H_2O]_3]^-$. The calculated absorption of $[H_2O]_3]^+$ at λmax=523nm(f=0.2146) and λmax=722 nm(f=0.1422) may contribute to the observation of colorful aurora.

Table 1. Molecular orbital modelings of ionosphere constituents of N_2 and H_2O

	λmax (nm) (intensity)	λmax (intensity)	E (kcal/mol)	ΔE (kcal/mol)	LUMO (eV)	HOMO (eV)
$N_2\&H_2O$	213.(0.0010)	152.(0.0125)	-116676.28	-	-1.16	-7.72
$[N_2\&H_2O]^-$	502(0.0012)	419.(0.0029)	-116639.66	36.62	7.08	4.3
$[N_2\&H_2O]^+$	830(0.0003)	434.(0.0006)	-116409.17	267.11	5.69	3.02
$N_2\&(H_2O)_3$	**195(0.0046)**	**194(0.0028)**	**-212596.68**	-	**-0.95**	**-8.01**
$[N_2\&(H_2O)_3]^-$	**614(0.0017)**	**304(0.0166)**	**-212576.35**	**20.33**	**5.69**	**3.02**
$[N_2\&(H_2O)_3]^+$	456(0.0010)	367(0.0111)	-212379.48	217.2	-4.82	-14.11
$H_2O)_2$	149(0.0445)	-	-95902.45	-	1.1	-7.21
$[H_2O)_2]^-$	603(0.1077)	448(0.1354)	-95829.4	73.05	7.89	5.31
$H_2O)_3$	147(0.0307)	-	-143861.99	-	1.66	-7.67
$[H_2O)_3]^+$	**722(0.1422)**	**523(0.2146)**	**-143623.76**	**238.23**	**-4.35**	**-15.64**

Figure 1. Spectrum of N_2 dischrge and UV/Vis absorption spectra of plasma-state N_2 and

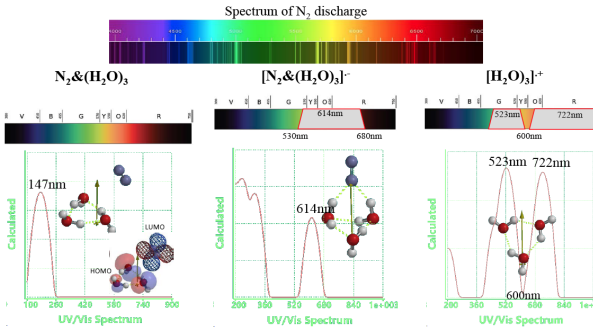

CONCLUSION

Molecular modeling suggests that green atmospheric aurora is caused by filtering by plasma-state N_2-water clusters, and the blue, yellowish or red aurora by filtering by plasma-state water clusters.

REFERENCES

[1] Wikipedia "Gas-discharge lamp", http://en.wikipedia.org/wiki/Gas-discharge_lamp.

[2] Hehre. W. J. Application of Graphical models in Book, A Guide to Molecular Mechanics and Quantum Chemical Calculation, Chapter 19, 473, Wavefunction, Inc. 2003.

Energy Saving Process of Organic Hydride for Hydrogen Energy by Using Microwave-Driven Catalytic Reaction

Satoshi Horikoshi

Department of Materials and Life Sciences, Faculty of Science and Technology, Sophia University, 7-1 Kioicho, Chiyodaku, Tokyo 102-8554, Japan
e-mail: horikosi@sophia.ac.jp

Keywords: Microwaves; Heterogeneous catalyst; Dehydrogenation; Hydrogen energy; Organic hydride

INTRODUCTION

Hydrogen is the most abundant element in the universe, yet on Earth it has to be produced first because it only occurs in the form of water and hydrocarbons. This implies that we have to expend energy to produce energy resulting in a difficult economic dilemma because ever since the industrial revolution we have become accustomed to consume energy at relatively low costs.

Japan has proposed a major target to reduce by 50 % the emission of the greenhouse gas CO_2 by the year 2050. The introduction of renewable energy sources is indispensable to achieve this goal. A hydrogen-based fuel cell technology should contribute considerably to achieving this goal. Accordingly, fuel cells have been the object of extensive studies in Japan. Certain public institutions (e.g., in the transportation sector such as buses) already make good use of fuel cells as a source of power. Moreover, private cars that drive using fuel cell technology (fuel cell vehicle: FCV) are already commercially available (Toyota Motor Co. since December 2014). As well, power supplied by fuel cells is widely used in Japanese houses. The hydrogen gas is first extracted from liquefied petroleum gas (LPG) and its energy is subsequently converted by the fuel cell system into electricity (Ene farm system, Panasonic Co). The process occurring in a fuel cell is exothermic, the heat from which is used to boil water that is then used in bathrooms, and in other household applications. Even now hydrogen energy permeates our daily activities.

This presentation describes efforts in producing hydrogen gas from organic hydrides using a microwave-assisted catalyzed process in the presence of a catalyst, which consisted of platinum particles supported on an activated carbon substrate (Pt/AC).

Principal features of this microwave-assisted organic hydride method are high product yields, response of high hydrogen evolution, restraint from inactivation of the catalyst, and most importantly energy saving. Hydrogen evolution from methane via the methane dry reforming process is also described.

RESULTS

The dehydrogenation of methylcyclohexane was compared with microwave heating and conventional heating with a ceramics heater and insulator (**Figure 1**). The packed Pt/AC catalyst particulates were heated by microwaves at 330 ºC for 1, which resulted in ca. 94 % dehydrogenation of methylcyclohexane occurring in less than 90 s. On the other hand, when using a ceramic heater, dehydrogenation at 330 ºC needed more than 30 min even though an insulator was used. Clearly, microwave heating led to hydrogen evolution in a much shorter time. On suspension of microwave irradiation, the catalyst particulates promptly cooled and hydrogen evolution stopped. In contrast, upon suspension of conventional heating with a ceramic heater, hydrogen gas continued to evolve for more than 30 min. The total power consumption of the microwave system was 36 W (microwave applied power, 17 W), while the ceramic heater expended 115 W. Evidently, microwave heating is also favored in terms of power consumption and thus an attractive and profitable energy saving system, in addition to the shorter times for hydrogen evolution. It should be recalled, however, that electric energy was used to produce hydrogen energy.

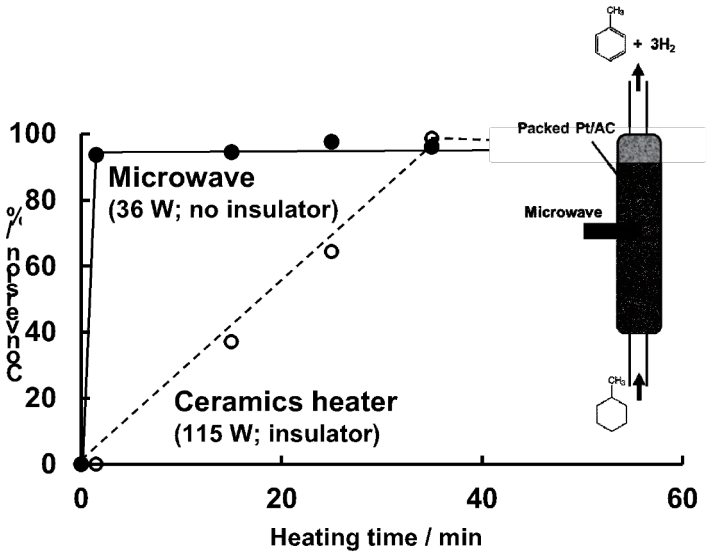

Figure 1. Dependence of the conversion of methylcyclohexane to hydrogen gas and toluene over the Pt/AC catalyst under microwave heating and conventional heating with a ceramics heater (temperature, 330 °C).

REFERENCES

[1] S. Horikoshi, N. Serpone (Eds) Microwaves in Catalysis – fundamental research and scale-up methodology (will be published 2015), Wiley-VCH Verlag GmbH, Weinheim, Germany.

Numerical Modeling of Microwave Heating of Porous Catalytic Bed

Pranjali Muley[1], Dorin Boldor[1]

[1]Department of Biological and Agricultural Engineering, Louisiana State University, Baton Rouge, USA.

Keywords: Numerical modeling, Microwave heating of porous material, catalytic upgrading of biofusection headings must be el

INTRODUCTION

Due to advances in microwave technology, microwave heating has gained popularity not only in the field of food processing but also organic chemistry, catalytic reactions and other industrial processes. Dielectric heating of catalyst bed has multiple advantages over conventional heating techniques such as increased heating rates, high heating efficiency and improved catalyst performance. Due to these potential advantages of microwave technology applied to chemistry, the technology is now extensively studied to investigate the effect of microwave heating of catalyst in endothermic reactions. In order to design an experimental set up for microwave heating of catalyst, it is important to understand how the catalyst can be heated in the microwave reactor. Studying the heating patterns of the catalyst bed in the microwave reactor can be helpful for the design of reactor and reaction parameters. The objective of this study is to develop a numerical model of electromagnetic heating of packed catalyst bed by coupling high frequency electromagnetism at 2450 MHz with heat transfer in porous catalyst bed reactor and to investigate the effect of size, shape and position of catalyst bed inside the microwave on the temperature attained and the overall heating profile.

METHODOLOGY

The dielectric properties of HZSM-5 powder was measured at nine temperatures ranging from 250° - 700 °K using an Agilent ENA series E5071C Network Analyzer (Agilent Technologies, Inc. Santa Carla, CA). A numerical model was developed using COMSOL Multiphysics 4.2 studying the effect of electromagnetic irradiation on porous catalyst bed. Main steps in model development were geometry generation, defining boundary and subdomain settings, mesh generation, solver definition, solving and post processing. Two shapes of catalyst bed a) block and, b) cylindrical and five different positions a) center of the waveguide, b) base of the waveguide (z=-0.03 m), c) upper edge of the waveguide z=0.03 m, d) z=-0.01 m and e) z=-0.02 m were studied. The effect of size of the catalyst bed was also tested by designing a smaller diameter tube while maintaining the volume of the catalyst bed. The new design was tested for 3 different positions a) center of the waveguide z=0, b) z=-0.01 and, c) z=-0.02 from the center.

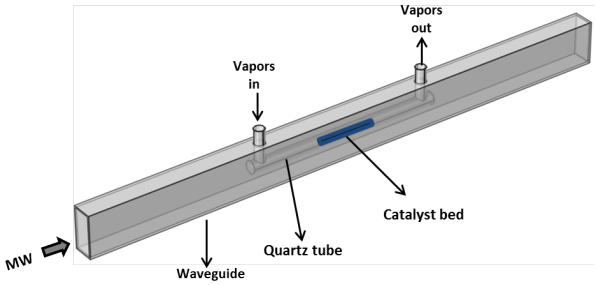

Figure 1. Geometry of microwave system used to heat porous catalyst bed

RESULTS

The electric field and temperature profile of a cylindrical porous catalyst bed placed at the center of the microwave reactor is shown in figure 1. The incident microwave power was 400 W.

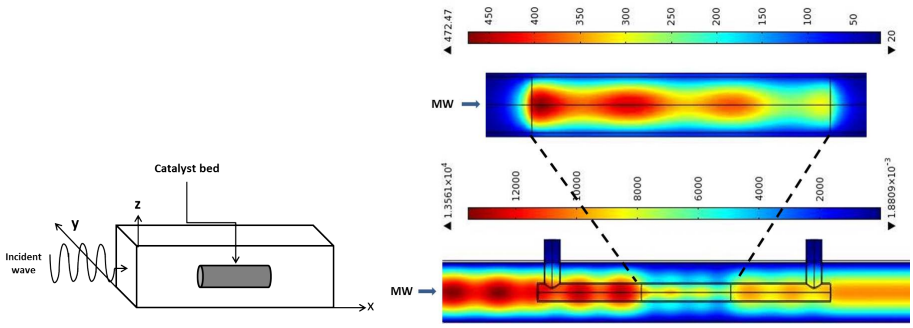

Figure 2 Electric field (V/m) and temperature profile for catalyst bed at the center of the cavity (z =0)

DISCUSSION

Brick shaped sample heats more uniformly compared to cylindrical sample. If the radius of the sample is decreased, while maintaining the volume of the sample, the microwaves penetrate deeper inside the sample, and more uniform heating is observed throughout the length of the sample. Samples placed 20 mm away from the center heat more uniformly compared to samples placed at the center, higher temperatures are achieved when the sample is placed 10mm away from the center. This is because stronger resonance effects occur due to disorderly wave reflections within the samples.

CONCLUSION

It was observed that the sample position, shape and size of the sample, all significantly affect the heating profile and temperature gradient inside the porous media heated using microwave irradiation. This type of numerical modeling can be used to optimize the process parameters and design an efficient process depending on the ease of operation, manufacturing, and cost efficiency.

Modeling-Based Optimization of Thermal Processing in Microwave Fixation

Ethan M. Moon[1], John F. Gerling[2], Charles W. Scouten[3], and Vadim V. Yakovlev[1]

[1]Department of Mathematical Sciences, Worcester Polytechnic Institute, Worcester, MA, USA
[2]Gerling Applied Engineering, Inc., Modesto, CA, USA
[3]NeuroscienceTools, Downers Grove, IL, USA

Keywords: Brain tissue, complex permittivity, dielectric insert, dissipated power, neurochemistry, uniform heating

The technology of microwave fixation has been identified as a highly promising (if not the only possible) way to lock the chemical state of the brain for post-sacrifice chemical analysis. This is a critical and challenging part of neurologic studies looking for cures for numerous disorders, including such degenerative diseases as Parkinson's and Alzheimer's [1-2]. Popular commercially available microwave fixation instruments use water jackets aiming to redistribute the electric field in the cavity in order to heat the animal's head uniformly. In such a configuration, however, the temperature field in the brain tissue is hardly controlled, whereas homogeneous thermal treatment is a requirement in this application. In this case, a significant fraction of the microwave power is absorbed by the water and thus wasted. Therefore, in order to rapidly heat a small volume occupied by the processed tissue (characterized by a lower loss factor), these systems need to use high microwave power (up to 5-10 kW). This suggests that existing equipment for microwave fixation is operationally cumbersome and energy inefficient, and thus motivates developing new efficient applicators for neurochemical studies.

In this paper, we report the results of initial exploration of an alternative microwave system design featuring a solid dielectic insert. The insert's shape and complex permittivity are determined for a given brain's material parameters and geometry so that the dissipated power distribution in the animal's head is as homogenious as possible. The corresponding optimization problem is formulated and solved with the use of a computational procedure using numerical data generated by a 3D model representing the microwave system.

We considered a fictional application, whose structure is conceptually similar to the GA5013 Microwave Animal Fixation System (Gerling Applied Engineering, Inc). The applicator consisted of a section of a single-mode rectangular waveguide, centrally connected with a cylindrical cavity of a diameter exceeding the wide wall of the

waveguide. The animal was positioned so that the body was in the cavity, and the head in the waveguide. The head was surrounded by a rectangular dielectric insert; on the side facing the input of the system, the insert was covered by a cone for improving the matching of the loaded applicator with a microwave generator.

The entire system has been reproduced in a 3D parameterized model built for the full-wave conformal FDTD simulator *QuickWave 2014* [3]. Since the process of microwave fixation is very quick (less than 1s), we assume that the time of heat transfer is negligible and our computation can be reduced to determination of dissipated power. In the model, the animal's body and head are approximated by a cylinder and a truncated cone, and we utilize the value of complex permittivity for a mouse brain (gray tissue) as $\varepsilon_m = 46.9 - j7.2$ [4] at 2.45 GHz. To ensure high solution accuracy, the scenario in the model is discretized with a non-uniform mesh (with max cell sizes of 5 mm in air and 1.5 mm in the insert and in the animal), and thus the model contains roughly 560,000 cells.

Systematic computational tests were performed for varying insert's heights and widths as well as dielectric constants and loss factors. These parameters were found to significantly influence the dissipated power distribution. Thus, they were used as design variables in the optimization problem, aiming to reach maximum uniformity of dissipated power in the brain tissue.

For a uniformity metric, we used the relative standard deviation (RSD) of the dissipated power in all cells within the truncated cone representing the animal's head. (A low RSD indicates that the data set has little variation, meaning it tends to have a uniform distribution.) Several local minima were found after a series of random simulations in the space of four design variables. We then formed a sub-space around a minimum by reducing the bounds of the original space and, through a dedicated sensitivity analysis, determined and dropped from the following calculations the two least-influential design variables. In the final stage, the sequential quadratic programming was used to determine the complex permittivity and shape of the insert corresponding to the lowest RSD.

Application of this optimization procedure with the chosen ranges of the design variables (including the range of dielectric constant of the insert exceeding ε_m') produced parameters of the system in which the RSD was reduced from 120-135% (in non-optimized designs) to 23-27%. The achieved level appears to be the best for the chosen sub-space of the design variables; however, optimization in other sub-spaces (in particular with the dielectric constant being less than ε_m') may provide solutions with lower RSD.

The procedure appears to be suitable for homogenizing dissipated power in other microwave applicators with high rates of thermal processing.

REFERENCES

[1] M. Davila, A.P. Candiota, M. Pumarola, and C. Arus, Minimization of spectral pattern changes during HRMAS experiments at 37°C by prior focused microwave irraditation, *Magn. Reson. Mater. Phys*., vol. 25, pp. 401-410, 2012.

[2] C. Mueller, S. Magaki, M. Schrag, M.C. Ghosh, and W.M. Kirsch, Iron regulatory protein 2 is involved in brain copper homeostasis, *J. of Alzheimer's Disease*, vol. 18, pp. 201-210, 2009.

[3] *QuickWave-3D*™, QWED Sp. z o. o., http://www.qwed.com.pl/.

[4] E.C. Burdette, F.L. Cain, and J. Seals, In vivo probe measurement technique for determining dielectric properties at VHF through microwave frequencies, *IEEE Trans. Microwave Theory and Tech*., vol. 28, no 4, 2003.

Dielectric Properties of Biomass and Biochar Mixtures for Bioenergy Applications

Candice Ellison[1], Samir Trabelsi[2] and Dorin Boldor[1]

[1]Louisiana State University, Baton Rouge, LA, USA
[2]Agricultural Research Service, Athens, GA, USA

Keywords: Dielectric mixtures, permittivity, dielectric constant, dielectric loss factor

INTRODUCTION

Biomass is an abundant and renewable energy resource, which may be converted into energy-dense products via thermochemical processing, namely pyrolysis and gasification, using microwave technology. However, before designing a microwave system suitable for thermochemical processing, a thorough understanding of a material's dielectric properties is useful since they are unique to individual materials and govern a material's response to microwave radiation. Dry biomass is a low dielectric loss material, and therefore cannot absorb enough energy to reach the high temperatures required by thermochemical conversion processes. Heating efficiency may be improved by doping the biomass feedstock with a microwave absorber, which is a material characterized by high dielectric loss. Biochar was investigated for microwave absorbing capabilities in this study; it is a byproduct of the thermochemical conversion of biomass, making it a cheap and convenient microwave absorber for this application.

METHODOLOY

The real (ε') and imaginary (ε") components of the complex permittivity were measured for different mixtures of biomass and biochar using an open-ended coaxial-line dielectric probe and a vector network analyzer over a frequency range of 500 MHz to 4 GHz. Dielectric data were collected for four biomasses (Southern pine, Chinese tallow tree, live oak, and energy cane) mixed with increments of 25% biochar up to 100% by weight. All samples had 12% moisture content by weight and particle sizes less than 500 µm. For each mixture, measurements were taken at different densities, which were obtained by compressing the sample into the sample holder with the end of the probe.

Figure 1. High temperature dielectric probe and stainless steel sample holder

RESULTS

The dielectric constant and dielectric loss factor measurements are presented as a function of biochar content (at 0.30 g/cm^3) and as a function density for energy cane biomass at 20°C and 2.45GHz. The experimental results indicate that dielectric properties are highly dependent on frequency, density, and the amount of biochar in the sample.

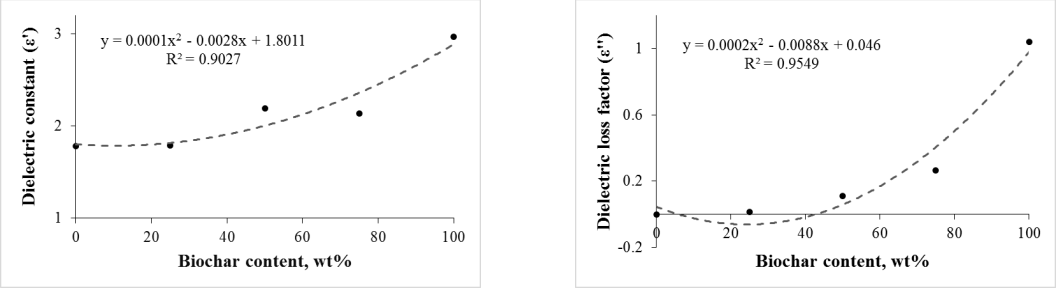

Figure 2. Dielectric properties of energy cane with different biochar contents normalized to a medium bulk density using the Landau-Lifshitz-Looyenga mixture equation at 2.45 GHz and 20°C.

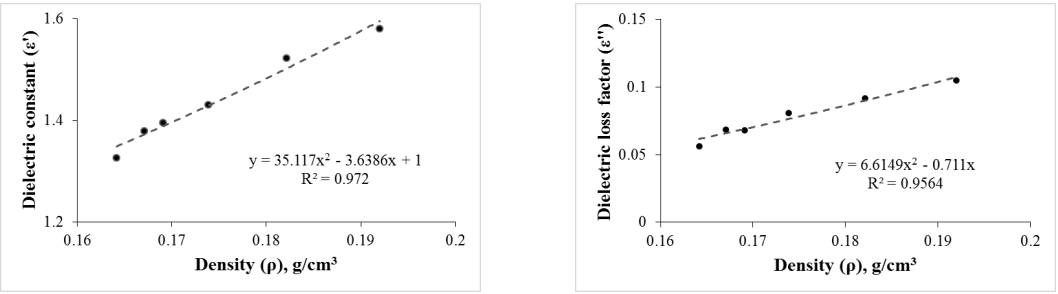

Figure 3. Dielectric properties a function of density for energy cane samples for energy cane (0% biochar) at 2.45GHz and 20°C.

DISCUSSION

The Landau-Lifshitz-Looyenga mixture equation was used to normalize the densities of the mixtures to the medium bulk density (0.30 g/cm^3). Both dielectric constant and dielectric loss factor increase as the percent weight of biochar increases in the mixture (Figure 2). Because biochar has a higher permittivity than biomass, the permittivity of the mixture increases as biochar content increases. Furthermore, the real and imaginary components of complex permittivity were observed to increase with the increase in bulk density (Figure 3). This is a result of the greater contact between particles in the mixture and reduction of air gaps with increasing density.

CONCLUSION

These data suggest that compressing the sample during microwave heating and adding biochar to biomass samples increases the dielectric properties of the samples, and thus, the microwave heating efficiency of biomass materials. The resulting permittivity data may be used to design microwave systems for thermochemical processing of biomass into bioenergy using biochar as a microwave absorber.

Thermal and Non-thermal Factors in Field-Assisted Powder Consolidation

Eugene A. Olevsky

San Diego State University, San Diego, USA

Keywords: Spark-Plasma Sintering, Microwave, Densification, Ponderomotive.

INTRODUCTION

Electromagnetic field-assisted powder consolidation accelerates densification and, in many cases, produces finer grains than regular hot pressing and sintering. Possible mechanisms of this enhancement of the consolidation in field-assisted versus conventional techniques of powder processing are identified and categorized with respect to their thermal and non-thermal nature.

FACTOR CATEGORIZATION

By and large, the difference between field-assisted sintering [1- 7] (e.g. spark-plasma sintering or SPS, microwave sintering, etc.) and conventional powder hot consolidation process outcomes can be attributed to the two categories of physical phenomena: (i) thermal and (ii) non-thermal. Thermal phenomena may include: high heating rates, which enable higher sinterability of the powder [2,3]; high local temperature gradients, which drive thermal diffusion; highly non-uniform local temperature distributions, which cause local melting within inter-particle contact areas; highly non-uniform macroscopic temperature distributions, which create thermal stresses intensifying dislocation creep.

The non-thermal phenomena may include: electromigration [2] and intensified diffusion in ionic conductors, electroplasticity mechanisms, ponderomotive forces, electromagnetic "pinch" effect, dielectric breakdown of oxide films (cleansing effect) and defect generation at grain boundaries.

Below we describe possible contributions of two thermal (high heating rates and high local temperature gradients) and one non-thermal (ponderomotive effects) phenomena.

CONTRIBUTION OF HIGH HEATING RATES AND HIGH LOCAL TEMPERATURE GRADIENTS

Previously obtained theoretical results [3] indicate the ability of conventional sintering and hot-pressing models to describe the acceleration of the densification and deceleration of the grain growth under high heating rate conditions, such as those utilized during SPS, without the explicit employment of the heating rate as an additional governing parameter. Olevsky and Froyen [3] quantitatively demonstrated that rapid heating should accelerate densification during sintering due to the early activation of

consolidation diffusion mechanisms (e.g grain-boundary diffusion) and due to the reduced time of the low-temperature stage of sintering when surface diffusion dominates.

In contrast to heating rates, the role of temperature gradients as independent governing parameters influencing the constitutive behavior during sintering may be significant. This is related to the Ludwig-Soret effect [4] of thermal diffusion, which causes concentration gradients in initially homogeneous two-component systems subjected to a temperature gradient. The thermal diffusion-based constitutive mechanism of sintering results from the additional driving force instigated by the spatially varying temperature gradient, which causes vacancy diffusion (as opposed to traditional "component mixing" in regular diffusion, thermal diffusion may separate components). This mechanism should be an addition to the free-surface curvature driven diffusion considered in conventional sintering theories.

CONTRIBUTION OF PONDEROMOTIVE EFFECTS

Ponderomotive effects contribute directly to densification and to the kinetics of single contact growth during microwave sintering [5-7]. A considerable free surface electromigration during microwave sintering in a polarized electromagnetic field occurs at inter-particle interfaces. It can be shown that the electromigration flux reaches its maximum near the inter-particle contact edge and it is equivalent to the compressive stress acting on the contact between particles. The compressive stress is proportional to the intensity of the electric field at the inter-particle neck and inversely proportional to the ratio of the grain-boundary and surface diffusivities. The electromigration matter transport can substantially accelerate the shrinkage rate during microwave sintering in comparison to conventional sintering.

CONCLUSION

A relevant research should describe the impact of the specific for field-assisted sintering constitutive mechanisms of thermal and non-thermal nature on the additional driving forces for consolidation, including densification and inter-particle neck growth. The outlined conducted research represented the first steps in this direction.

REFERENCES

[1] R. Orru, R. Licheri, A. M. Locci, A. Cincotti, G. Cao, Consolidation/synthesis of materials by electric current activated/assisted sintering, Mater. Sci. Eng. R 63, 127–287(2009)
[2] E. Olevsky and L. Froyen, Constitutive modeling of spark-plasma sintering of conductive materials, Scripta Mater., 55, 1175-1178 (2006)
[3] E. Olevsky, S. Kandukuri, and L. Froyen, Consolidation enhancement in spark-plasma sintering: Impact of high heating rates, J. App. Phys., 102, 114913-114924 (2007)
[4] E. Olevsky and L. Froyen, Influence of thermal diffusion on spark-plasma sintering, J. Amer. Ceram. Soc., 92, S122-132 (2009)
[5] K. I. Rybakov, E. A. Olevsky, E. V. Krikun, Microwave Sintering: Fundamentals and Modeling, J. Am. Ceram. Soc., 96, 1003–1020 (2013)
[6] E.A. Olevsky, A.L. Maximenko, and E.G. Grigoryev, Ponderomotive effects during contact formation in microwave sintering, Modelling Simul. Mater. Sci. Eng., 21, 055022 (2013)
[7] K. Rybakov, E. Olevsky, and V. Semenov, Microwave ponderomotive effect on ceramics sintering, Scripta Mater., 66, 1049-1052 (2012)

Microwave Heating of Gold Nanoparticles for Gout Treatment

Muzaffer Mohammed; Yehnara Ettinoffe; Bridget Kioko; Taiwo Ogundolie; Morenike Adebiyi; Nishone Thompson; Brittany Gordon and Kadir Aslan.

Morgan State University, Department of Chemistry, 1700 East Cold Spring Lane, Baltimore, USA

Keywords: Gout, Microwave Assisted De-Crystallization, metal colloids.

INTRODUCTION

Uric acid is produced in the human body by catabolism of purine-rich food. Over-burdening of the kidney due to continuous filtering of serum and fluids leads to accumulation of uric acid in joints, which is known as hyperuricemia or gout [1, 2]. In this condition, uric acid crystallizes in synovial joints leading to a restricted joint movement and severe inflammation [2]. In this paper, we show the results of a novel technique based on low power microwave heating in conjunction with gold or silver colloids to successfully dissolve uric acid crystals in an in-vitro experimental design replicating synovial joints.

METHODOLOGY

Figure 1 shows various steps in uric acid de-crystallization. In brief, a modified glass surface was deposited with collagen fibers followed by attaching a silicone isolator to replicate the closed joint environment. Synovial fluid was added to a well along with uric acid solution and incubated for 1 hour. Gold or silver colloids were then added to the well and the entire setup was microwaved for 1-10 min using 100 W power (PL 1 in 900 W microwave). Optical images were collected after every heating cycle to monitor the impact of heating on the uric acid crystals.

RESULTS

Figure 2 shows before and after images of control and test wells. Control experiments show no change in the quantity and size of uric acid crystals whereas using gold colloids and low power (80-100 Watts) microwave heating for 10 min, ~80 % of the uric acid crystals were dissolved. Use of silver colloids instead of gold colloids did not show any significant reduction in uric acid crystal quantity or impact their size.

DISCUSSION

The significant decrease in the quantity of uric acid crystals after microwave heating indicates successful destruction of the crystals in the synovial fluid through microwave-induced rapid movements of metal colloidal particles. The colloids, along with dissolved uric acid, could be retrieved *in-vivo* though a minor extraction procedure similar to cerebro-spinal fluid (CSF) extraction from the spinal cord.

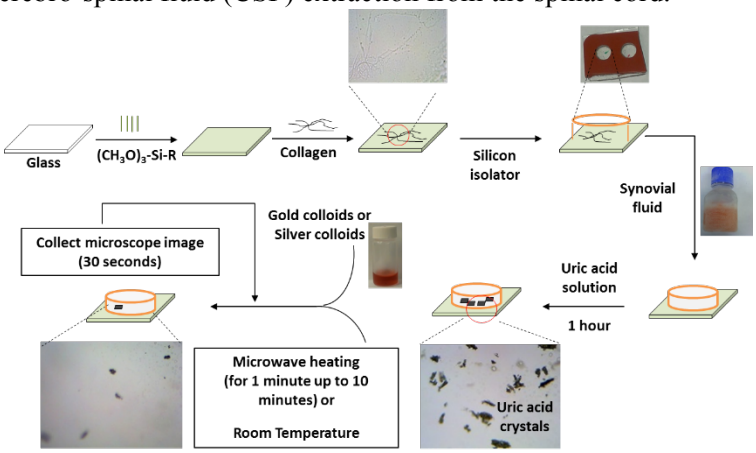

Figure 1. Schematic depiction of uric acid de-crystallization technique using microwave heating.

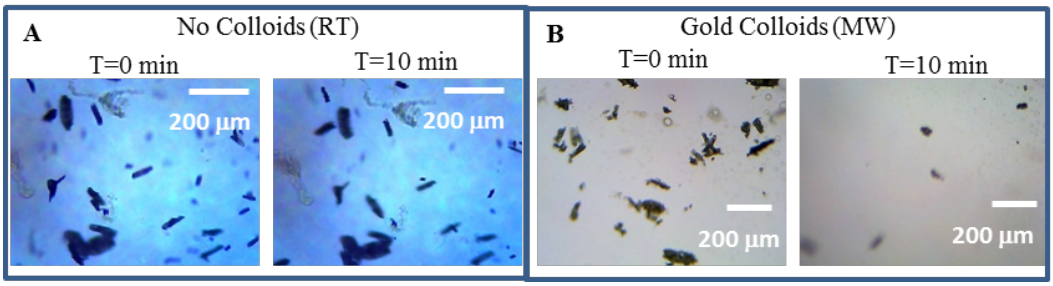

Figure 2. Optical images of uric acid crystals at (A) room temperature without colloids (B) after addition of gold colloids and using microwave heating.

CONCLUSION

The outcome of this research demonstrates the potential application of low power microwave heating with gold colloids has potential to be minimally invasive alternate treatment for gout.

REFERENCES

[1] M. B. Davidson, S. Thakkar, J. K. Hix, N. D. Bhandarkar, A. Wong, and M. J. Schreiber, "Pathophysiology, clinical consequences, and treatment of tumor lysis syndrome," *The American journal of medicine,* vol. 116, pp. 546-54, Apr 15 2004.

[2] J. E. Seegmiller, A. I. Grayzel, L. Laster, and L. Liddle, "Uric acid production in gout," *The Journal of clinical investigation,* vol. 40, pp. 1304-14, Jul 1961.

β-SiC Nanoparticles Produced with Microwaves at 2.45 GHz and 5.8 GHz

Karina A. Cabriales-Gómez, Juan A. Aguilar-Garib

Universidad Autónoma de Nuevo León, FIME, San Nicolás de los Garza NL, Mexico

Keywords: β-SiC, nanoparticles, microwaves, pyrolysis, PTMS, TEOS.

INTRODUCTION

Nanoparticles of SiC have been synthesized by a modified sol-gel process for preparing two polymeric precursors, pheniltrimethoxysilane (PTMS) and tetraethoxysilane (TEOS) with a phenolic resin, followed by microwave pyrolysis, either in vacuum or under N_2, aimed to produce the cubic polytype 3C-SiC. Production of this carbide, known as β-SiC, without the hexagonal (H) or rhombohedral (R) polytypes, was accomplished at 2.45 GHz in both single mode and multi-mode cavities [1-3]. However, the same tests conducted at 5.8 GHz with a corresponding cavity and waveguide gave controversial results regarding the production of this carbide [4] because fewer nanoparticles were produced and it was difficult to locate them for characterization. The purpose of this research was to elucidate if β-SiC is produced at 5.8 GHz.

METHODOLOY

The first polymeric gel, based on PTMS, was prepared with 40 g of $PhSi(OCH_3)_3$, 10.90 g of H_2O, 12.92 g of CH_3OH, and 0.36 g of HCl. The solution was stirred for 30 min and condensed to produce an arrangement of silane with Si-O-Si bonds. A gel containing silicon and carbon was formed after adding 12 ml of NH_4OH and leaving the solution resting for 5 minutes.

A gel based on TEOS was prepared with 41.66 g of $Si(OC_2H_5)_4$, 14.41 g of H_2O, 36.85 g of CH_3CH_2OH and 0.36 g HCl. After one hour stirring, a condensate containing silicon but not carbon was produced. Hence it was necessary to add 54.16 g of Bakelite that was dissolved ultrasonically for 30 min in 162.48 ml of CH_3COCH_3 and then stirred 1 hour more. The gel was also formed after adding 12 ml of NH_4OH. Both gels were dried for 24 hours at 80 °C.

Samples of 0.7 g of either the PTMS or TEOS gel was placed in an alumina crucible for conducting the pyrolysis with microwaves using a bar of silicon carbide as a heating susceptor in a waveguide, or a cavity, in a N_2 atmosphere The samples were exposed to 200, 300, 400 and 500 W of microwaves at 2.45 GHz and 5.8 GHz. Exposition times were 5, 10 and 15 min. SiC was used in this work as the microwave susceptor, instead of graphite employed in an earlier research [1], in such a way that it did not chemically interact with the sample, to ensure that the necessary carbon for producing SiC nanoparticles was coming only from the precursors.

RESULTS AND DISCUSSION

Figure 1 shows the TEM images of PTMS obtained at 5.8 GHz. Si-C bonding was identified by FTIR, while the β-SiC lattice was confirmed by TEM with high-resolution images so that the interplanar spacing was measured. β-SiC has a characteristic peak at 36º (2θ, λ=1.54 Å) while the most common H polytypes have multiple peaks, and R polytypes have different peaks that could be identifiable for large particles, but the background hides the peaks with nanoparticles, hence the spots of electron diffraction are used for identifying the lattice.

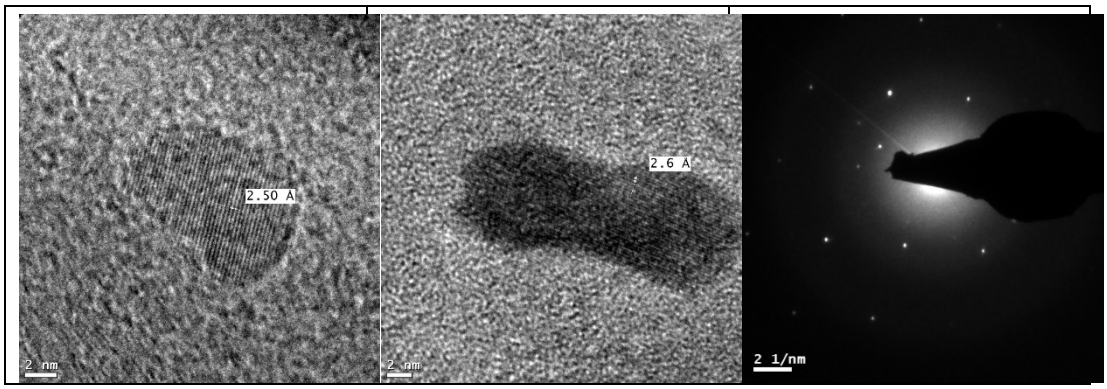

Figure 1. Nanoparticle of β-SiC produced with PTMS at 5.8 GHz and a clean electron diffraction pattern of the central image.

CONCLUSION

It was confirmed, by Transmission Electron Microscopy, that microwave pyrolysis of precursors produced by sol-gel, from PTMS and TEOS, at 2.45 and 5.8 GHz under different conditions, produce β-SiC.

REFERENCES

[1] J. Aguilar, L. Urueta, Z. Valdez, Polymeric synthesis of silicon carbide with microwaves. *Journal of Microwave and Electromagnetic Energy*. Vol. 40, No. 3, 2007, pp. 145-154.

[2] J. A. Aguilar-Garib, K. Cabriales-Gómez, M. Garza-Navarro, Characterization of silicon carbide nanoparticles obtained by microwave pyrolysis, 13th International Conference on Microwave and High Frequency Heating, Toulouse, France, September 5- 8th, pp. 26-29, 2011.

[3] J. Aguilar-Garib, K. Cabriales-Gómez, N. Villalón-Juárez, Microwave Pyrolysis of Sol-Gel Prepared Precursors for Synthesis of SiC Nanoparticles. *44th Annual Microwave Symposium, Denver CO (July 2010)*, pp. 89-94.

[4] K. Cabriales-Gómez, J. A. Aguilar-Garib, 5.8 GHz microwave synthesis of SiC nanoparticles from sol-gel precursors, 14th International Conference on Microwave and High Frequency Heating, Nottingham, UK, September 16- 19, pp. 180-183, 2013.

ACKNOWLEGEMENT: The authors express their gratitude to the Mexican Council for Science and Technology (CONACYT), and the PAICYT, a research program of the UANL.

Automotive Microwave Plasma Ignition Comes of Age

Roger A. Williams[1] and Dr. Yuji Ikeda[2]

[1]NXP Semiconductors, Smithfield, RI, USA
[2]Imagineering, Inc, Kobe, Japan

Keywords: Automotive applications, microwave plasma, ignition, impedance matching, semiconductor, LDMOS.

INTRODUCTION

Over the past decade, many efforts have been undertaken to improve the efficiency and reduce the emission of greenhouse gases in automotive internal combustion engines. Microwave plasma ignition has been shown to have great potential in expanding the limits of lean-burn and exhaust gas recirculation (EGR) technologies necessary for improving fuel economy, particularly in its ability to stabilize combustion and initial flame development [1].

Several automobile manufacturers have concluded that the performance and reliability of this technology has now reached a level where it is suitable for use in production vehicles. As a result, attention has now shifted to engineering challenges related to microwave transistor and amplifier development, packaging, spark plug design, and plasma control techniques. In this paper we describe microwave plasma ignition technology, review the improvement in engine performance achieved with current technology, and discuss practical system implementations and a variety of engineering innovations in architecture, antenna design, plasma control, and amplifier packaging that have finally brought microwave plasma ignition to the automobile assembly line.

MICROWAVE PLASMA IGNITION TECHNOLOGY

For practical reasons, the most complete development on plasma ignition has involved plasma-assisted combustion in gasoline engines, using microwaves to pump plasma seeded by a standard spark discharge from an ignition coil. In this technology, special spark plugs are used which include both a standard spark gap and a (generally coaxial) microwave radiator [2]. The paper also summarizes recent developments using only a microwave spark plug, without need for a high-voltage spark.

RF energy emitted into the engine cylinder is absorbed by the free electrons in the spark discharge, generating non-thermal plasma. Microwaves are applied as a burst of narrow pulses to keep gas temperature low in order to reduce NO_X generation [3]. This microwave-generated plasma stabilizes the combustion of leaner, higher-EGR gas mixtures than can be supported by spark discharge alone. Microwave pumping intensifies

flame propagation, supporting plasma combustion at pressures above 1 MPa and high flow velocities. The paper discusses the plasma physics in more detail and illustrates plasma generation with high-speed schlieren and conventional videos.

ENGINE PERFORMANCE

The current fuel efficiency improvement (integrated over a JC-08 drive profile) in a production engine is 13% ISFC (indicated specific fuel consumption) vs. stoichiometric, which results in 9% BSFC (brake specific fuel consumption) vs. stoichiometric with the stock vehicle powertrain. This is a 5% higher BSFC than can otherwise be achieved with non-plasma lean-burn and EGR technology.

PRACTICAL IMPLEMENTATIONS

The paper describes practical implementations of the system architecture, control electronics, power amplifiers, plasma control methods, spark plugs and matching structures. One example of innovation is the new triaxial spark plug shown in figure 1, designed to improve the efficiency of plasma generation by exciting a greater volume.

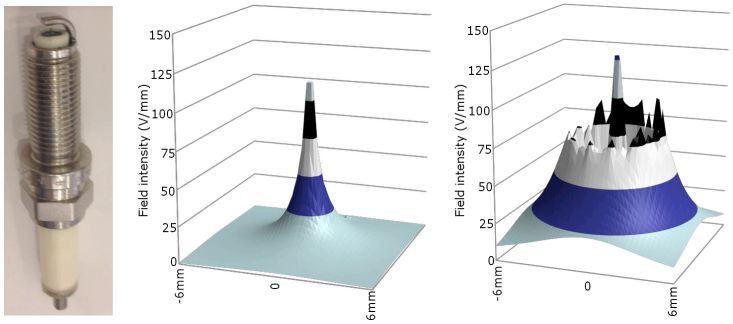

(a) (b) (c)

Figure 1. New triaxial microwave + HV spark plug: physical plug (a) and simulated field intensity (at 1 kW power) of the conventional coaxial plug (b) and new triaxial plug (c).

CONCLUSION

Over the past four years, automotive microwave plasma ignition has matured from promising laboratory experiments to production-ready technology. We can expect to see the first vehicles benefiting from the technology on the road within a few years.

REFERENCES

[1] K. Linkenheil, H. Ruoß, T. Grau, J. Seidel, and W. Heinrich, "A novel spark-plug for improved ignition in engines with gasoline direct injection (GDI)," *Plasma Science, IEEE Transactions on*, vol. 33, no. 5, pp. 1696–1702, 2005.

[2] A. Nishiyama and Y. Ikeda, "Improvement of lean limit and fuel consumption using microwave plasma ignition technology," SAE Technical Paper, Tech. Rep., 2012.

[3] A. DeFilippo, S. Saxena, V. Rapp, R. Dibble, J. Y. Chen, A. Nishiyama, and Y. Ikeda, "Extending the lean stability limits of gasoline using a microwave-assisted spark plug," SAE Technical Paper, Tech. Rep., 2011.

Market Trends in High Power Microwave Technology for Industrial Microwave Heating and Plasma Applications

Klaus-Martin Baumgaertner

Muegge GmbH, Reichelsheim, Germany

Keywords: Microwave Heating, Low Pressure Microwave Plasma, Atmospheric Pressure Microwave Plasma, Switch Mode Power Supply

HIGH-POWER INDUSTRIAL MICROWAVE HEATING

INTRODUCTION

Microwaves facilitate targeted heating of a large variety of materials used in industry, be it homogeneous heating from the core to the surface or focused heating of a selected area or volume. This is a big advantage compared to conventional heating that is restricted to heating of the surface of materials. New developments particularly in power supply technology are aimed at meeting the challenges of industrial microwave heating.

HIGH-POWER INDUSTRIAL MICROWAVE HEATING: MARKET TRENDS AND APPLICATIONS

An increasing number of industrial heating processes are sensitive to overheating and therefore require specific control technologies. In order to avoid overheating, microwave power supplies with extremely short response times are required. These short response times cannot be met by linear power supplies. Therefore, the new switch mode power supply (SMPS) technology is gaining increasing market share.

State-of-the-art single microwave heating units provide microwave power in the range of 300 W up to 30 kW at 2.45 GHz and between 5 kW and 100 kW at 915 MHz. In the near future, single 915 MHz microwave heating units are expected to supply a maximum power of 125 kW. Operation of several microwave heating units in parallel easily meets the requirements of industrial microwave heating processes. Applications can be found in vacuum drying, sterilization and pasteurization in the food industry, in manufacturing of multilayer timber panels in the woodworking industry, in focused activation of chemical reactions in the pharmaceutical industry and in the manufacturing of insulating materials for sound absorption and for energy saving, respectively, in the construction materials industry for example.

HIGH-POWER INDUSTRIAL MICROWAVE PLASMA TECHNOLOGY

INTRODUCTION

Microwave-induced plasmas are another large application area of industrial microwave technology. At low pressure conditions, non-equilibrium plasmas are formed by microwave plasmas. They are characterized by the predominant excitation of electrons, i.e. the formation of "hot" electrons, while the heavy ions and neutral particles in the plasma stay almost at room temperature. As a consequence, plasma surface treatment of even thermal sensitive materials is feasible. Additionally, high electron densities inducing high densities of radicals are achievable by microwave plasmas. As a consequence, high etching and deposition rates, respectively, can be obtained.

HIGH-POWER INDUSTRIAL MICROWAVE PLASMA TECHNOLOGY: MARKET TRENDS AND APPLICATIONS

The Remote Plasma Source (RPS) operated at low pressure is characterized by a high radical density outside of the plasma chamber. As a result, the RPS is applied for e.g. selective, fast and highly efficient plasma etching of semiconductor and organic materials, in particular. RPS etching rates of more than 200 µm/h can be achieved for organic materials like SU-8 photo resist.

Duo-Plasmaline plasma sources are another type of microwave plasma sources providing highly efficient and fast plasma etching of different kinds of materials. However, their major field of application is plasma deposition. Prominent examples are:

- scratch resistant layers deposited by high-rate plasma processes with deposition rates higher than 50 µm/min for transparent polymers used in the construction material and in the automotive industry,
- highly impermeable gas and water vapor barrier films in the nano-range required for example in food packaging as well as for encapsulation of thin-film solar cells and even organic light emitting diodes (OLEDs),
- passivation layers in photovoltaics as well as
- artificial diamond for a variety of applications.

Microwave power supplies based on the newly developed switch mode power supply (SMPS) technology can easily be pulsed to enlarge the parameter space in order to improve the quality of the surface modified in the plasma process.

Atmospheric pressure microwave plasmas can be used to form both non-thermal plasmas like at low pressure and thermal plasmas. While the non-thermal plasma of the Micro Plasma Jet is applied e.g. for efficient inside cleaning of long but narrow cannulas, the thermal plasma of the an Atmospheric Plasma Source (APS) is very well suited for abatement of waste gas containing fluorinated and chlorinated volatile organic compounds (VOCs), for rapid activation of different kinds of surfaces and for deposition of amorphous layers for application in photovoltaics for example.

Industrial Usage of Plasma Chemical Vapor Deposition to Manufacture Optical Glass Fibers

Mathé van Stralen, Ton Breuls, Igor Miličević, Hans Hartsuiker and Gertjan Krabshuis

Draka Comteq Fibre B.V. (Prysmian Group), Eindhoven, The Netherlands

Keywords: Microwave plasma, PCVD, Glass Fibers, Industry.

INTRODUCTION

Optical glass fibers are drawn from a preform, which is a quartz rod of typically more than 1m long and up to 20cm in diameter, depending on the final application (e.g. telecom, datacom and sensors). The refractive index profile of the final glass fiber is already present in this preform. The diameter of the glass in the fiber is standardized at 125µm. During the draw, two protective polymer coatings and possibly a colored ink are added, resulting in a fiber with a diameter of about 250µm. There are several methods to manufacture the preform. It is common that the inner part (i.e. the core rod) is made in a different way than the outer part. It contains the refractive index profile for optimized light guidance. High quartz quality is required to obtain low attenuation, typically 0.18 dB/km at 1550nm. The core rod consists of the core, a cladding where the light presence is still non-negligible, and possibly a trench for obtaining low bending loss for the fiber. Depending on the application, the quartz volume of the inner part varies between only 3% and 35% of the total preform volume. The outer part mainly contains quartz and mainly cost determines the choice of manufacturing method. For this, the Applied Chemical Vapor Deposition (APVD) process was developed, in which pure sand is guided into a radio-frequency plasma flame directed at the core rod, which results in overcladding the core rod with pure quartz. For the core rod, microwave plasmas was used to deposit (doped) quartz on the inside of a very pure substrate tube. This process is known as Plasma Chemical Vapor Deposition (PCVD). After the PCVD, the tube with a thick deposition on the inner surface was collapsed into the core rod. This paper aims to elucidate the PCVD process and to discuss microwave issues in a continuous production environment.

PCVD PROCESS

Figure 1 sketches the industrial set-up. At the start, a very pure quartz substrate tube was mounted in a PCVD lathe. One side was connected to the gas-supply, while the other to a vacuum pump. A mixture of process gasses flowed through the substrate tube at low pressures (typically 10-20 mbar). The gasses $SiCl_4$ and O_2 were used to build the quartz network, while $GeCl_4$ and C_2F_6 were added as dopants to raise or to lower the refractive index, respectively. The substrate tube was positioned inside a microwave applicator in order to create a plasma which enhances the chemical reaction. The tube temperature was kept high (typically 1000-1200°C) in order to avoid bubble formation during the succeeding collapsing process. The microwave CW power was in the range of 5-10 kW. The applicator moved back and forth (up to 0.5 m/s) in order to uniformly deposit many ~1µm thin quartz layers along the tube.

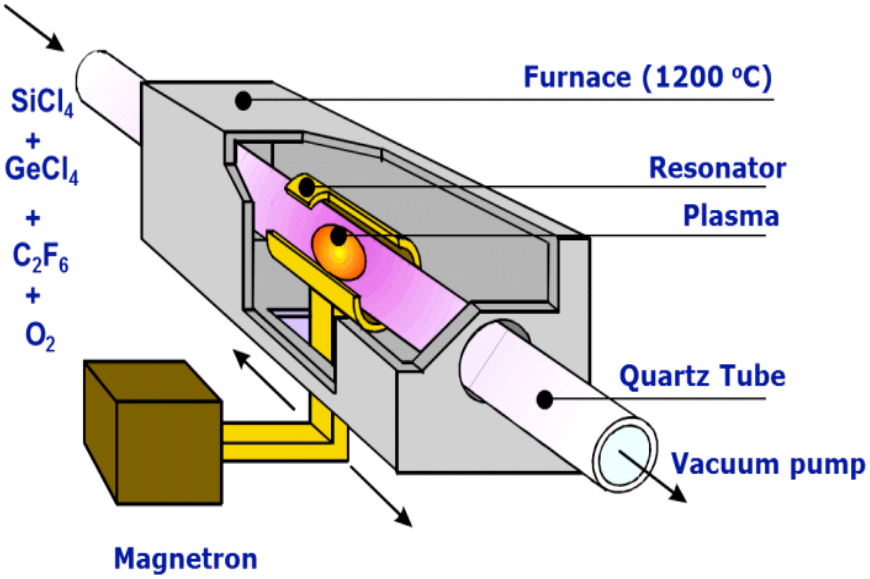

Figure 1. Schematic diagram of the industrial PCVD lathe

RESULTS

By controlling the gas mixture for each layer, the radial profile was controlled very accurately. Combined with the high reproducibility of the process, products which require accurate index profiles [2] can be made. The plasma deposition also allowed high incorporation efficiencies which is very important for the multimode products which require a lot of the expensive $GeCl_4$. Additionally, high incorporation of Fluorine is also possible, so that low refractive indices were also reachable. The microwave system was very important for the accuracy and reliability of the system. It must also withstand the harsh environment (i.e. high temperature, high power and quick (de)acceleration in the turning points). Special attention was paid to the interaction of the microwaves with the surroundings to accurately control the index.

CONCLUSION

High power microwave equipment was successfully used to fabricate optical glass fibers during continuous production at several factories around the world for some decades. In contrast to traditional alternative methods, the PCVD process needs only 1 step to create silica glass and has the ability to deposit many thin layers to control the index profile, which results in accurate refractive index profiles.

REFERENCES

1. A. H. van Bergen and T. Breuls, PCVD: The Ultimate Technology for Production of High Bandwidth Multimode Fibres, *International Wire & Cable Symposium Proceedings*, pp. 66-71, 1998
2. D. Molin, F. Achten, M. Bigot, A. Amezcua-Correa, P. Sillard, WideBand OM4 Multi-Mode Fiber for Next Generation 400Gbps Data Communications, *International Wire & Cable Symposium Proceedings*, pp. 366-369, 2014

Microwave-Induced Plasma Analysis: Experiment and Modelling

M. Andrasch[1], M. Baeva[1], A. Boesel[1], J. Ehlbeck[1], D. Loffhagen[1], U. Schnabel[1] and K.-D. Weltmann[1]

[1]Leibniz Institute for Plasma Science and Technology, Greifswald, Germany

Keywords: microwave plasma, plasma simulation, plasma diagnostic

INTRODUCTION

The development of atmospheric pressure microwave plasma sources has opened a wide range of new applications. Most of them are based on high density of charged particles and active species combined with low thermal load. To design and optimize applications and plasma sources the knowledge of plasma parameters and the electromagnetic field distribution is indispensable. Therefore, experiments have been conducted with complementary microwave plasma sources and diagnostics. These were accompanied by self-consistent 2-D fluid models to provide an inside view of the plasma sources. This contribution overviews the performed analysis of microwave-induced plasmas, and presents selected results concerning the involved fundamental processes.

METHODOLOY

Due to the small dimensions of atmospheric pressure microwave plasma sources and their sensitivity to additional diagnostic ports, experimental determination of localized plasma parameters is not always possible. On the hand, there are optical methods (figure 1a) with high spatial resolution but weak sensitivity to low density of charged particles. However, 40 - 200 GHz microwave based methods are very sensitive to low electron densities but lack spatial resolution (figure 1b). To get a full view, a combination of diagnostic results with a model covering the whole source is promising. The present work implemented a self-consistent fully coupled spatially two-dimensional time dependent fluid model.

Based on these methods, a MiniMIP microwave jet plasma with absorbed powers to 20 W in Argon at atmospheric pressure was analyzed (figure 2a) [1]. Furthermore, the start-up behavior of a PLexc® microwave plasma torch working at Argon pressures from 5 mbar to 80 mbar, with incident powers up to 300 W was investigated (figure 2b) [2]. In both cases, interaction of the microwave field with electrons was modeled and particles densities, fluxes and temperatures were quantified.

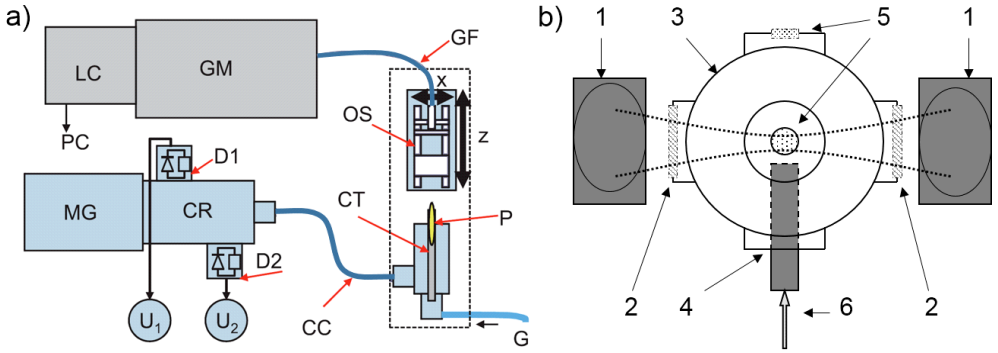

LC: line camera, GM: grating monochromator, GF: glass fiber, OS: optical system, P: plasma, CT: ceramic tube, D1,D2: diodes, CR: circulator, MG: magnetron, CC: coaxial cable, G: gas inflow

1: elliptical mirror, 2: teflon window, 3: vacuum vessel, 4: plasma source, 5: view port (silica glass), 6: gas inflow

Figure 1. (a) shows the experimental setup (optical Emission spectroscopy) of the microwave plasma jet. (b) depicts the experiment concerning the microwave plasma torch (microwave interferometry).

RESULTS

One important result of the analysis of the MiniMIP microwave plasma jet was the identification of the molecular ion Ar_2^+ as a major ion species (figure 2a) in some regions. The observed contraction of the discharge is explained by the strong nonlinear temperature dependence of the reaction kinetics through the gas dynamics. A significant outcome of the investigation on the PLexc® microwave torch is the simulation of the dynamic interaction of the electromagnetic field and plasma (figure 2b).The induced plasma changes time dependent the field geometry, which than effects the local plasma heating. Based on this dynamic behavior a higher absorption of microwave energy was observed in comparison to the steady state. Furthermore, the electron temperature increases to 2 eV during the start-up.

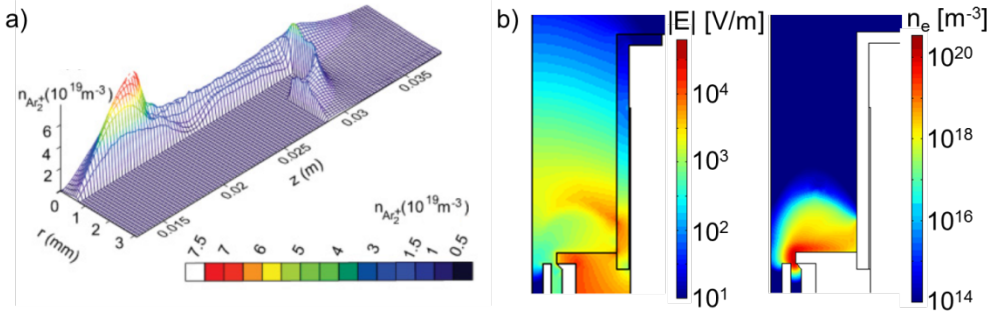

Figure 2. (a) shows the spatial distribution of the molecular ion Ar_2^+ of MiniMIP. (b) diagrams a snapshot during the start-up of the electric field strength and the electron density inside PLexc®.

REFERENCES

[1] Baeva M, Bösel A, Ehlbeck J and Loffhagen D "Modeling of microwave-induced plasma in argon at atmospheric pressure" *Physical Review E* 2012 **85** 056404

[2] Baeva M, Andrasch M, Ehlbeck J, Loffhagen D and Weltmann K-D "Temporally and spatially resolved characterization of microwave induced argon plasmas: Experiment and modeling" *Journal of Applied Physics* 2014 **115** 143301

Pragmatic Water Permittivity Model

Vladimir Bilik[1,2]

[1]Slovak University of Technology, [2]S-TEAM Lab, Bratislava, Slovak Republic

Keywords: Complex permittivity model, microwave materials, water properties.

INTRODUCTION

A number of publications, e.g. [1] – [9], provide values of the complex relative permittivity of water $\varepsilon_r = \varepsilon' - j\varepsilon''$ that are valid over certain ranges of frequency, temperature and salinity. The values of ε_r are given directly or in terms of the Debye model constituents ε_s, ε_∞, τ and conductivity σ, and are often accompanied by approximation formulae. There are some practical difficulties in using such composed data in electromagnetic simulators, including: (1) discrepancies in data from different authors; (2) intervals of validity that do not fully cover the range of interest; (3) some data presented only in tabular form; and (4) multi-tier approximating formulas that are too complicated to be entered into the simulators although the resulting dependencies are smooth, and are thus amenable to simple and easily implementable polynomial approximation. Thus, as an attempt to eliminate the above difficulties, we propose here a simple polynomial model based on a compromise between selected representative sources. Models for two ISM bands (915 and 2450 MHz) have been created that are valid for common tap water (salinity 0.033%) in the temperature range 5 to 95 °C.

METHODOLOGY AND RESULTS

The following procedure has been adopted to create the models:

1. Temperature dependencies $\varepsilon'(T)$ and $\varepsilon''(T)$ were computed using the original source procedures. Sources [1] – [9] were chosen for the analysis. Model [1] was modified by adding the conductivity term $-j\sigma/(\omega\varepsilon_0)$ to the Debye formula; the water conductivity σ was computed according to [2]. The results were displayed in common graphs (an example for 2450 MHz is shown in Figure 1).

2. Based on visual comparison of these graphs, a compromise, average *master table* was constructed for both ε' and ε'', spanning the range 5 to 95 °C.

3. The master tables were approximated by $y(T) = a_0 + a_1T + a_2T^2 + a_3T^3$ where y is either ε' or ε'' and T is in °C. The coefficients are summarized in the table below.

f (MHz)	Quantity	a_0	a_1	a_2	a_3
915	ε'	87.27	-0.36437	4.3757E-4	0
	ε''	8.68	-0.21351	2.6700E-3	-1.1560E-5
2450	ε'	84.17	-0.27483	-3.3526E-4	0
	ε''	22.02	-0.61682	7.0286E-3	-2.8494E-5

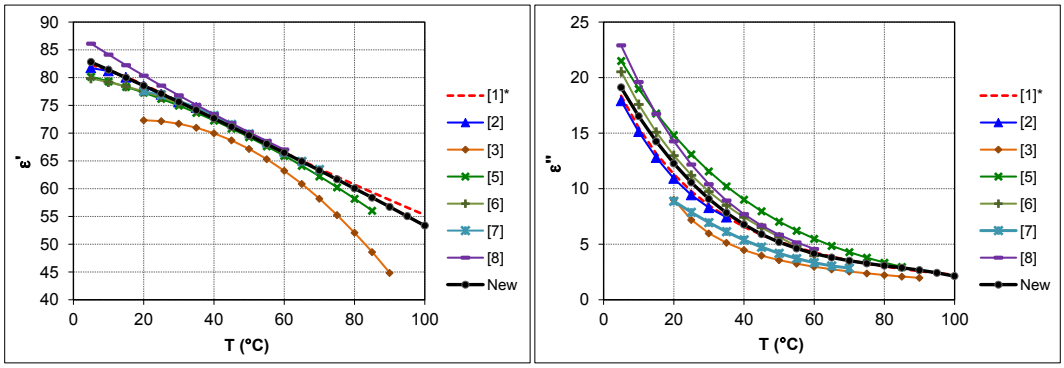

Figure 1. Real and imaginary parts of complex permittivity of tap water at 2.45 GHz. Results of the proposed model are labeled *New*.

The used polynomial degrees are sufficient to ensure the RMS approximation deviations below 0.02, which is at least an order of magnitude less than the data dispersion of the original sources.

CONCLUSION

The obtained polynomials are easily programmable into electromagnetic simulators. The complex permittivity they provide is a good compromise, valid in a temperature range sufficiently wide for most applications.

REFERENCES

[1] P. O. Risman and B. Wäppling-Raaholt, Retro-modelling of a dual resonant applicator and accurate dielectric properties of liquid water from -20 °C to +100 °C, *Measurement Science and Technology*, vol. 18, pp. 959-966, 2007.

[2] L. A. Klein and C. T. Swift, An improved model for the dielectric constant of sea water at microwave frequencies, *IEEE Journal of Oceanic Engineering*, vol. OE-02, No. 1, pp. 104-111, 1997.

[3] V. V. Komarov, Closed-form representation for temperature-dependent dielectric and thermal properties of microwaveable substances, *Proc. 47th IMPI Microwave Power Symp., Providence, RI, USA, June 2013*, pp. 30-35.

[4] V. V. Komarov and J. Tang, Dielectric permittivity and loss factor of tap water at 915 MHz, *Microwave and Optical Technology Letters*, vol. 42, No. 5, pp. 419-420, 2004.

[5] A. Von Hippel, *Dielectric materials and applications*, MIT Press, Cambridge, MA, 1954.

[6] F. Franks (ed.), *Water. A comprehensive treatise, Volume 1*. Plenum Press, New York, 1971.

[7] G. Farrell, W. A. McMinn, and T. R. Magee, Dielectric and thermal properties of pharmaceutical powders, *Proc. 10th Int. Conf. on Microwave and RF Heating, Modena, Italy, 2005*.

[8] P. Ratandecho, K. Akoi, and M. Akahori, The characteristics of microwave melting of frozen packed beds using a rectangular waveguide, *IEEE Trans. Microwave Theory and Tech.*, vol. 50, No. 6, pp. 1495-1502, 2002.

[9] J. N. Ikediala et al, Development of a saline water immersion technique with RF energy as a postharvest treatment against colding moth in cherries, *Postharvest Biology and Technology*, vol. 24, pp. 25-37, 2002.

Small-Sample Positional Effects in Microwave Ovens

Robert F. Schiffmann

R.F. Schiffmann Associates, Inc., New York, USA

Keywords: Sample placement, microwave ovens, test procedures, small samples.

INTRODUCTION

It is known that microwave ovens vary in performance in many different ways, not simply due to their wattage output. For example, earlier work by this author [1] indicated that some lower power ovens might heat small samples more rapidly than higher wattage ovens. The phenomenon of "hot" and "cold" spots in microwave ovens has also been known for many years. Recently, while testing as part of an investigation of a microwave injury, extreme temperature differences were seen in small samples of the same size and containing the same materials, but located at different positions on the glass turntable. Campden BRI [2] showed that the location of field maxima on microwave oven turntables vary in different ovens and that the center of the turntable, just above the driveshaft, can be either a "hot" or "cold" spot, while at the edge of the turntable it is then likely to be just the opposite. It is the purpose of this paper to demonstrate these variations and to demonstrate that the need to accurately place samples in the same location for every test is essential in order to achieve reproducible results.

METHODOLOGY

Tests were performed by heating 50 g samples of Canola Oil in small polypropylene cylindrical containers [(5.0 cm (height) x 1.2 cm (diameter)] for 60 seconds in each of three different microwave ovens, and each case the sample was placed either in the exact center of the turntable or at a location 5 cm from the turntable edge. The three ovens used in these tests were:

- GE Spacemaker II JEM31SF001 (~700 watts)
- Sharp Carousel R4A78 (~900 watts)
- KitchenAid KCMS1515RBL-1 (~1000 watts)

Note that the wattages shown are approximate averages of several IEC 705 tests. Also, prior to running tests in any oven, it was first tested by that procedure. Following each test, the turntable was removed from that oven and placed in a room temperature water bath for at least three minutes so as to prevent any confounding of the results due to heat transfer from the turntable. Great care was taken to place the samples in exactly the same location on the turntable test-to-test.

RESULTS

The results of the earliest tests are shown in Table 1.

OVEN	LOCATION ON TURNTABLE	START TEMP. (C)	FINAL TEMP (C)	Δ T (C)
GE	CENTER	23	163	123
"	EDGE	23	71	30
SHARP	CENTER	23.8	76.3	34.8
"	EDGE	23.8	94.5	52.9
KITCHENAID	CENTER	26.5	128.9	84.7
"	EDGE	26.5	111.4	84.7

Table 1: Effect of placement of 50-gram sample of Canola Oil in 3 different microwave ovens.

DISCUSSION

The results of these tests, and many others not shown but with the same or similar materials, demonstrate the sensitivity of placement of small samples in order to achieve reproducible results. This is especially necessary in order to avoid errors comparing temperatures measurements when heating non-aqueous materials, of lower specific heat capacity, on the order of 0.5 calories/gm*°C or less. It is not unusual to see differences of 50° to over 100 °C between two samples: one in the center and the other near the edge of the turntable.

CONCLUSION

In order to reproduce results heat transfer results with 95% confidence, and in order to avoid large temperature discrepancies when performing tests on small samples, i.e. 50 grams or less, especially on non-aqueous materials of lower specific heat capacity, i.e. 0.5 calories/gm*°C or less, the samples must be placed in the same location, with a precision of 10 mm on the turntable or oven-floor in a non-turntable oven. Other handling steps must be taken as well, such as cooling the glass turntable between each test, in order to avoid heat transfer from a hot turntable confounding the results.

REFERENCES

[1] R.F. Schiffmann, Problems in standardizing microwave oven performance, *Microwave World*, vol. 11, no 3, pp 20-24, 1990.

[2] G. Hooper, Food reheating instructions – a key element in delivery of safe, high quality foods, Campden BRI Report, 2014.

How to Make a Microwave Vacuum Dryer with a Turntable

R.L. Monteiro[a], B.A.M. Carciofi[a], J.B. Laurindo[a] and A. Marsaioli Jr.[b]*

[a]Department of Chemical and Food Engineering, College of Food Engineering, Federal University of Santa Catarina (UFSC), EQA/CTC/UFSC, 88040-900, Florianópolis, SC, Brazil
[b]Processing Engineering Group, Food Technology Institute, 13070-178, Campinas, SP, Brazil

Keywords: microwave vacuum drying, equipment, freeze drying, bananas, food quality.

INTRODUCTION

A domestic microwave oven was adapted in order to operate as a microwave vacuum dryer with turntable. The dryer performance was assessed with 5 mm thick slices, dried under vacuum at three different levels of microwave power: 400, 700 and 1000 W. The experimental results showed that it is possible to produce dried bananas with similar characteristics as those obtained from a freeze-drying (FD) process, but taking much shorter process times, i.e. 20 minutes against 10-12 hours. The system developed in this work is a low cost, flexible and ease-to-assemble device, which can be easily made from domestic microwaves. It allows microwave vacuum drying (MWVD) of fruits and vegetables at lab scale, but can be the basis for making larger equipment. Vacuum drying is particularly suitable for products that are sensitive to heat, such as fruits with high sugar content and certain vegetables with high added value [1]. Microwave heating under vacuum improves the efficiency of drying and prevents or reduces oxidation, preserving product color, texture and flavor, leading to products with quality compared to freeze-dried products [2]. The use of turntable during the drying process is important to improve the quality of the dried fruits as a result of fast and more uniform heating. Literature reports many studies on MWVD of fruits and vegetables, like banana [3], among others, although these studies did not report the use of turntables. The new device was tested for drying banana slices, which were also freeze-dried in order to compare processes and products.

MATERIALS AND METHODS

Bananas (*Musa sapientum L.,* Prata variety) were selected based on their ripeness, solid content and resistance to penetration. Selected samples had soluble solids content of 22.5 ± 1.6 ^{o}Brix and penetration resistance of 5.9 ± 1 N. The selected fruits were manually peeled and cut into 5 mm thick slices, the fruit edges being discarded. A microwave oven of 45 liters volume, 2.45 GHz, 1000 W maximum power (Electrolux, model MEX55, Brazil) was chosen for making the dryer. A polypropylene container was used as the vacuum chamber, which was connected to the vacuum line through a rotary joint. Figure 1 shows the adapted microwave oven. A lab size freeze-dryer (Liotop, model L101, Brazil) was used for the FD operation.

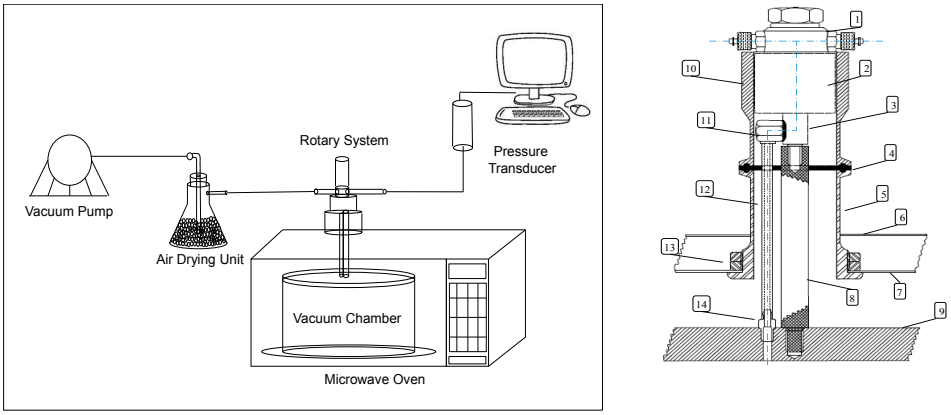

(a) (b)

Figure 1 Schematic diagram of the microwave vacuum dryer: (a) over-all system representation; (b) cut view of the rotary joint system.

RESULTS AND DISCUSSION

The Table 1 below shows the mean moisture contents (± s.d.) of samples for MWVD processes, under 400, 700 and 1000 W magnetron power, before and after drying, together with respective water activities values (± s.d.). The drying times were 27.67, 17.67 and 13.67 min, respectively. The value of FD drying time is also shown for comparison. These results indicate clearly the huge potential of microwave vacuum drying for many applications.

Table 1 Drying Results of MWVD and FD Processes

MWVD Load: 85.55±0.69g/Power,W:	Mean Moisture, d.b., $g.g^{-1}$±s.d.		Water activity, a_w±s.d.		Drying times, min.
	Before drying	After drying	Before drying	After drying	
400	2.28±0.14	0.019±0.007	0.981±0.004	0.207±0.062	27.67
700	2.28±0.14	0.030±0.017	0.983±0.003	0.262±0.066	17.67
1000	2.40±0.10	0.034±0.003	0.981±0.006	0.259±0.006	13.67
FD Load: 2000±0.1g	2.28±0.14	----------	----------	----------	780

CONCLUSION

The MWVD process with a turntable is a useful tool for investigating the application of MWVD to any food, including fruits and vegetables. Banana slices dried by MWVD exhibited structures very similar to those produced by FD, with very short drying times and, probably, at much lower costs. The turntable improved the quality of final product due to uniform heating.

REFERENCES

[1]M. Zhang, J. Thang, A.S. Mujumdar, S. Wang. Trends in microwave related drying of fruits and vegetables. *Trends in Food Sci. & Tech.*, vol.17, pp.524-534, 2006.
[2] S. Gunasekaran. Pulsed microwave-vacuum drying of food materials. *Drying Technology*, vol.17, pp.395-412, 1999.
[3] N. Mousa and M. Farid. Microwave vacuum drying of banana slices. *Drying Technology*, vol.20, pp.2055-2066, 2002.

A Solid State High Power Microwave Generator for Industrial Applications

Kenneth Kaplan[1], Manuel F. Romero[2]

[1]Cellencor, Inc., Ankeny, IA, USA
[2]NXP Semiconductors, Smithfield, RI, USA

Keywords: Microwave generator, solid state, LDMOS, semiconductor, heating, drying

INTRODUCTION

The Raytheon Corporation introduced the first high power microwave generator for industrial use over 40 years ago. Current generators operate in the 896/915 MHz ISM band and utilize magnetron tubes to produce either 75 or 100 kW. “Cooker” CW magnetrons have a long list of disadvantages including: a short lifetime, expensive replacement cost, instability, fragility, and limited power control capabilities.

The improved power control, replacement cost and life-time of solid state amplifiers makes this technology a competitive alternative to magnetron based generators. In this work, the first LDMOS-based solid-state 50kW microwave generator was developed to replace magnetron generators in the 902-928 MHz ISM band.

ARCHITECTURE OF THE GENERATOR

The architecture of the 50kW generator was built around 32, 1.6 kW capable, LDMOS power amplifier [PA] modules. The modules feed a radial combiner which provided a single waveguide output. A two-stage 800W pallet was developed to serve as the building block for the 1.6 kW modules (see Figure 1). To generate 1.6 kW per module, two dual-path 800W pallets were combined using a 4:1 combiner (see Figure 1).

A robust distributed control system was utilized. Each module had an embedded microcontroller that managed and monitored the amplifiers. A local network connected the modules to the main system controller. The generator could be operated and monitored over Ethernet by a programmable logic controller (PLC) or a plant distributed control system (DCS).

RESULTS

The initial module-level performance is summarized in Table 1.

Table 1. Measured CW RF performance for single module at 20° C cold-plate temperature

Frequency (MHz)	Output Power (W)	Drain Efficiency (%)	Gain (dB)	Drain Voltage (V)	Drain Current (A)
915	1645	55.4	34.4	50	59.4

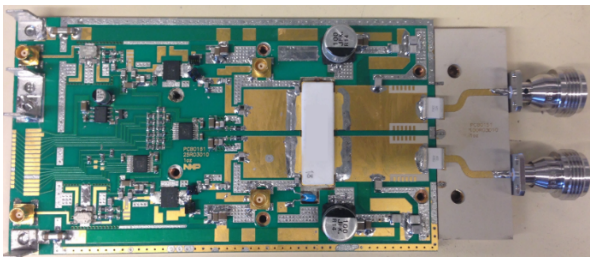

Figure 1. Single 800W pallet

DISCUSSION

Compared to current magnetron generators, the solid state unit has many advantages including lower life-time cost of ownership, higher reliability, ease of maintenance, and greater safety. Perhaps the most significant new feature of the solid state generator is the extreme controllability of its output power. The amplifier modules are driven by a modulated exciter, permitting high-speed software-driven power and modulation control. As a result, the generator can deliver continuous power, pulsed power, pulse-width modulated power, or any other software-synthesized waveform.

There has been research suggesting that fast pulsed power modes may provide significant benefits in improving the efficiency and effectiveness of heating and cooking systems [1]. Use of these modes has not been possible with magnetron driven generators; availability of a solid state microwave generator will give scientists and engineers a new tool to innovate as well as improve cooking, heating and drying processes.

CONCLUSION

The availability of high performing LDMOS amplifiers has enabled the development of solid-state microwave generators for use in industrial heating. The benefits of real-time power and signal control will facilitate the development of improved heating algorithms while providing significant operational and economic benefits.

REFERENCES

[1] S. Gunasekaran and H.W. Yeng, Effect of experimental parameters on temperature distribution during continuous and pulsed microwave heating, *Journal of Food Engineering*, vol. 78, pp. 1452–1456, 2007.

Comparative Leakage of Transparent Conducting Film Etalon Windows and Standard Metal Grid Windows

Raymond L. Boxman[1] and Sergey Shchelkunov[2]

[1]Tel Aviv University, Tel Aviv, and ClearWave Ltd., Herzliya, Israel
[2]Yale University, New Haven CT, U.S.A.

Keywords: microwave oven window, microwave etalon, transmission measurement.

INTRODUCTION

Domestic microwave ovens have a door with a microwave attenuating metal grid observation window. Visibility of the oven contents, however, is greatly hampered by the grid. Windows with transparent conducting coatings has been suggested for many years[1], but are not commercially produced. Recently a low cost configuration based on commercially available glass panes coated with transparent conductive oxide coatings and arranged in an etalon configuration was presented[2], and the leakage using an optimized configuration was demonstrated to be less than with conventional windows[3]. However the repeatability of the measurements was limited by magnetron drift and changing of the water load characteristics with heating. The objective of the present work was to compare the etalon and grid windows under comparable conditions.

METHODOLOY

A window was assembled using Pilkington TEC5 glass, with a nominal sheet resistance of 5 Ω. Two TEC5 panes were arranged like a sandwich with the conductive coating facing outward, and the uncoated surfaces contacting a plane glass inner pane. The conductive coatings were separated by 12.4 mm of glass, forming a ~λ/4 etalon at 2.45 GHz, in the glass.

Two types of tests were performed to compare the etalon and grid windows. In the first test, samples of each window were placed between two waveguides, with 82×164 mm cross-sections and 82 mm length. The waveguides were equipped with monopole probe antennae, which were connected to the appropriate ports of a network analyzer to determine the transmission coefficient (S21) through the sample. In the second test, a 20 liter oven was fitted alternatively with either its original grid window, or the etalon window. A 82×164 mm cross-section rectangular waveguide was abutted to the outer surface of the window. The monopole antenna was connected to the input of a spectrum analyzer. The oven was either empty, or loaded with 300 ml of tap water at room temperature, in a 400 ml beaker. The oven was operated at full power, and at either

20 s or 55 s from the beginning of operation, a series was initiated of 8132 sweeps, each of 1 ms duration and 100 MHz width, centered on 2.45 GHz. The spectra, averaged over the 8132 sweeps, was displayed, and integrated by the spectrum analyzer over the 100 MHz region to determine the band power.

RESULTS

The results of the first test are shown in Table 1. It may be seen that the attenuation of the etalon window was 15.6 dB (i.e. ×36) better than the standard grid window.

Table 1. Transmission coefficient of standard grid and ClearWave Etalon windows

CONFIGURATION	S21 (dB)
base - no window	-5.2
with standard grid window	-41.8
with 12.4 mm glass etalon	-57.4
etalon - grid	***-15.6***

Spectral analysis revealed that most of the power was emitted from the oven in a 50 MHz region centered on the nominal 2.45 GHz frequency. The leakage power, integrated over a 100 MHz band centered at 2.45 is shown in Figure 6 for three situations with both the original grid and etalon windows. In each situation, the leakage band power was significantly less (by 5-10 dB) with the ClearWave etalon window.

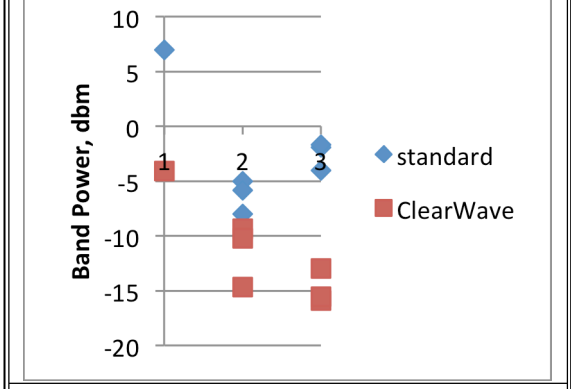

Figure 1. Band power under the following conditions: 1) empty oven, after 20 s operation, 2) 300 ml load, after 20 s operation, and 3) 300 ml load, after 55 s operation.

DISCUSSION AND CONCLUSIONS

Both tests show that the etalon window provided better microwave leakage attenuation than the original grid window, as well as providing vastly better visibility. While both the metal grid and elaton windows provide sufficient attenuation to meet current safety standards, we may anticipate efforts to lower the maximum allowable leakage, for example to interfere less with communications (e.g. WiFi and Bluetooth) using the 2.45 GHz ISM frequency. Most important, the etalon window allows 'cook and look' feedback to assist the consumer in correctly preparing food.

REFERENCES

[1] [1] D.B. Haagensen, Microwave Ovens, U.S. patent 2,920,174, 5 Jan. 1960.
[2] [2] R. Boxman, V. Dikhtyar, E. Gidalevich, V. Zhitomirsky, "Microwave oven window", U.S. Patent 8,772,687 B2, 8 July 2014.
[3] 3 R.L. Boxman, E. Yaari, V. Dikhtyar, E. Gidalevich, V. Zhitomirsky, "Clear etalon windows for domestic microwave ovens: analysis and measurement", International Microwave Power Institute Annual Symposium, Denver, 14-16 July 2010.

Economics of Solid-State Power Amplifiers for High Volume RF Energy Applications

Klaus Werner

RF Energy Alliance, Beaverton, Oregon 97003 USA
www.rfenergy.org

Keywords: Solid state RF power amplifiers, RF energy applications, economics, very high volume production, RF Energy Alliance introduction.

INTRODUCTION

An ever-increasing performance/price ratio coupled with unprecedented, precise radio frequency (RF) signal control expands practical use cases for solid-state RF technology to include heating and power delivery scenarios. The technology is making inroads into application fields that were previously considered impossible for tube-based systems (e.g. automotive ignition [1], medical imaging and cancer treatment [2]) and into high barrier markets (e.g. industrial [3] and consumer microwave furnaces) currently dominated by cost-effective magnetrons.

The new markets present ultra-high volume opportunities for businesses operating directly and peripherally in the RF technology industry. They also present alternative revenue potential to that of maturing markets such as cellular infrastructure. Hence, the attractiveness of these new markets is enormous. The "only" issue lies in the fact that the current cost structure for reasonably powerful solid-state RF systems is prohibitive to consumer markets. It is this last topic that the RF Energy Alliance [4] has set out to resolve. To eventually win against the magnetron, solid-state RF systems must be price-competitive—next to its undisputed control advantages.

DISCUSSION

In what follows, we will consider the example of a consumer microwave oven to detail the challenges for a broad application of RF solid-state technology. Goal is the complete replacement of the magnetron tube inside the furnace, enabling a huge improvement of user experience and a wealth of possible differentiation in the appliance's functionality. Figure 1 below depicts the modules of an RF generating sub-system for RF energy systems. The main part of concern lies with the high power amplifier. The rest of the sub-system is more or less standard and has previously experienced very high volume manufacturing and consumer business orientation.

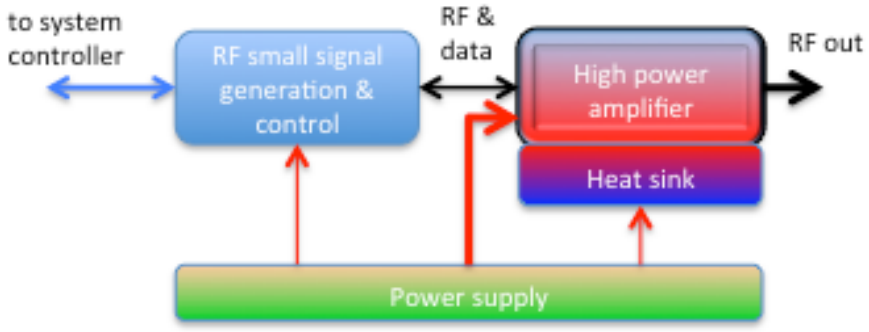

Figure 1. Block diagram of a solid state RF generator sub-system with modules

The RF power amplifier, however, needs to see a cost reduction of roughly a factor of 20. This is a tough target, but manageable.

For once, the sheer available volume helps. Investments into manufacturing and device technology need to be done, but can be motivated with volume numbers at the right time. This is no small feat: with more than 70 million microwave ovens sold per year around the world, this market alone would exhaust today's annual production of RF power semiconductor devices.

Reliability requirements between the current professional and future consumer markets differ by about a factor of 100. The current designs "for eternity" will be replaced by designs, which are good enough for 3000 hours of operating life. This allows higher operating temperatures of the PA electronics, reduced cooling requirements, less reliable underlying technologies and the like. Clearly, adapting reliability to the needs will help in cutting cost—for some components by as much as a factor of 5 to 10. We believe a particular challenge lies in the recruitment of RF power designers who can, at the same time, also handle the stringent cost targets.

Another, more technical challenge lies in the design of very efficient amplifiers. Devices based on laterally diffused metal oxide semiconductor (LDMOS) technology are leading so far, but GaN might prove to be a stiff contender if its prices drop. At system level, the benefit of a higher efficiency PA multiplies via smaller power supplies and less dissipated heat. In any case, a minimum overall efficiency of 54 percent should be met; otherwise the appliance could not be sold in China, for example.

It should be noted, however that a solid state based microwave really shines in characteristics like user experience, reproducibility and cooking results. The Alliance is hence also working to establish new criteria, which are better suited towards the evaluation of these new systems.

CONCLUSION

The RF Energy Alliance members are convinced that the solid-state RF energy technology will be successfully introduced in very high volume, consumer-oriented markets in the near future. The organization is addressing the necessary economical, technological, regulatory and organizational elements to facilitate a breakthrough, which will benefit various applications and markets like lighting, automotive ignition and medical ablation in addition to microwave cooking.

REFERENCES

[1] K. Werner, H. Heuermann, A. Sadeghfam, The potential of RF Energy for the Ignition of Microplasmas, *High Frequency Electronics*, November 2012, pp. 38 – 43.

[2] J.F. Bakker, M.M. Paulides, A.H. Westra, H. Schippers, and G.C. van Rhoon, Design and test of 434MHz multi-channel amplifier system for targeted hyperthermia applicators, *Int. J. Hyperthermia*, vol. 26, no 2, pp.158 – 170, 2010.

[3] M.Mehdizadeh, Engineering and scale-up considerations for microwave induced reactions, *Res. Chem. Intermed.*, vol. 20, no 1, pp. 79-84, 1994.

[4] www.rfenergy.org

Waveguide Fabrication Methods to Meet Extreme Requirements

John F Gerling

Gerling Applied Engineering, Inc., Modesto, USA

Keywords: microwave; waveguide; fabrication methods; coordinate measuring machine

INTRODUCTION

The development of microwave heating applications often requires careful selection of the microwave source and design of the cavity, while most waveguide requirements can be met using generic components. Waveguide performance requirements are usually high and easily met as are specifications for geometric accuracy in simple designs. However, achieving both high performance and geometric accuracy can be challenging with complex designs. Unique designs and manufacturing methods may be required for extremely complex waveguide configurations.

METHODOLOY

Extremely complex waveguide configurations may be required where the microwave source and heating cavity are separated by a complicated network of system hardware through which the waveguide must pass. This is analogous to a vehicle exhaust pipe (Figure 1) that must pass from the engine to the rear. Multiple formed bends and flexible bellows sections are common for exhaust piping but for waveguide may be impractical.

Figure 1. Complex shapes of typical automobile exhaust pipes.

Figure 2 illustrates a waveguide section designed with multiple corners to fit through a similarly complicated space in a process system. In this particular case the complexity disallows the use of formed bends and flexible sections, while the close fit requires non-standard corner elbows in most places.

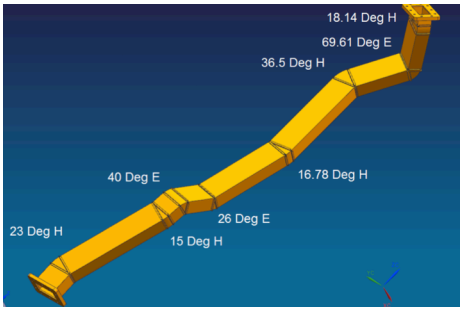

Figure 2. Complex waveguide section.

Waveguide elbow sections are usually fabricated using cast elbows that are designed to minimize input VSWR and commercially available in standard 30, 45 and 90 degree sizes. However, the tooling cost for cast elbows makes them impractical for the non-standard elbows shown in Figure 2.

Instead, these elbows were fabricated as machined halves using a double miter design [1] as illustrated in Figure 3.

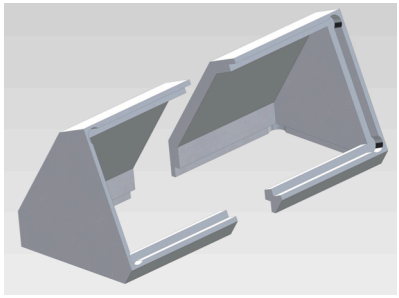

Figure 3. Double-miter machined E-plane elbow.

Aluminum dip brazing is a common method of waveguide fabrication to minimize insertion loss [2]. Due to the annealing and tempering processes involved, achieving close geometric tolerances required the use of fixtures (Figure 4) for both pre-braze tack-up of the assembly and post-braze machining of the flange faces.

Final performance optimization may require impedance tuning to reduce input VSWR and/or special interior surface treatment to reduce insertion loss.

Figure 4. Waveguide fixture used for pre-braze tack-up and post-braze machining.

RESULTS

Due to the extremely tight space through which these waveguide sections pass, all include a specified geometric profile tolerance of 1 mm (+/-0.5 mm) overall. Using a coordinate measuring machine (CMM), all surfaces on the entire assembly were inspected to verify the final geometry (Figure 5). Performance measurements using a vector network analyzer indicate <1.1 input VSWR and <0.1 dB insertion loss without impedance matching or special surface treatment.

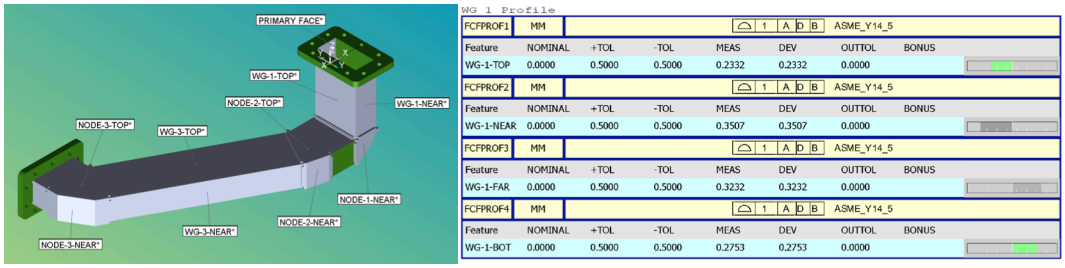

Figure 5. Waveguide surfaces to be inspected and sample CMM data.

CONCLUSION

High performance complex waveguide sections having extremely close tolerance geometric specifications can be manufactured using unique fabrication methods and careful inspection throughout the manufacturing process.

REFERENCES

[1] T. Moreno, *Waveguide Transmission Design Data*, McGraw-Hill, New York, 1948.
[2] *Fabrication of Rigid Waveguide Assemblies (Swept Bends and Twists)*, Military Standardization Handbook, MIL-HDBK-660B, US Dept of Defence, 2012.